ABSTRACT

AKDEMIR, KEREM ZIYA. Assessing Risks for New England's Wholesale Electricity Market from Wind Power Losses during Extreme Winter Storms. (Under the direction of Dr. Jordan Kern).

In the United States, the New England power grid and wholesale electricity market face unique difficulties from severe winter weather. During periods of extreme cold, the New England grid can experience dramatic increases in the market price of electricity due to a combination of high natural gas prices (greater heating needs and regional pipeline constraints) and higher electricity demand. In recent years, a significant amount of offshore wind power capacity has been planned for the region, and previous studies have shown potentially significant benefits specifically during winter cold snaps, including lower emissions and market prices. However, there has been limited consideration of potential wind power losses during severe winter storms due to wind speeds that are higher than the designed cut-out speed of the turbines, which would lead to a sudden loss of wind power when grid resources are already stressed. In this study, we develop an open-source power system model of the New England bulk electricity grid and use it to explore future wind power development in the region and assess risks associated with a sudden loss of wind during winter storms due to excessively high wind speeds. Results suggest that, quantified in terms of contribution to wholesale market price spikes, cut-out events in winter months caused by excessive wind speeds represent a relatively minor risk compared to the loss of wind power due to low wind speeds and sudden drops in wind speeds during summer. Overall, the benefits of having offshore wind power during winter weather events appear to significantly outweigh the risk associated with rare cut-out events during cold snaps.

Assessing Risks for New England's Wholesale Electricity Market from Wind Power Losses during Extreme Winter Storms

by
Kerem Ziya Akdemir

A thesis submitted to the Graduate Faculty of
North Carolina State University
in partial fulfillment of the
requirements for the degree of
Master of Science

Natural Resources

Raleigh, North Carolina
2021

APPROVED BY:

_____	_____
Dr. Jordan Kern Committee Chair	Dr. Gregory W. Characklis
_____	
Dr. Jeremiah Johnson	

DEDICATION

I dedicate this thesis to my wife, Ece, and my family. Thank you for your never-ending love and invaluable support.

BIOGRAPHY

Kerem Ziya Akdemir was born in Ankara, Turkey on August 16, 1995. He spent most of his childhood in Ankara and started to be interested in environmental issues. He wanted to improve himself in every field that could be a part of making the world a better place. With this goal in mind, he received Bachelor of Science degree in Environmental Engineering from Middle East Technical University in June 2018.

After his graduation, he worked at two companies on environmental impact assessment (EIA) reports of renewable energy projects, carbon abatement projects, voluntary carbon markets, emission trading systems (ETS). He got experienced in providing consultancy services to various firms on the carbon market as well as preparing emission monitoring plans. He is interested in the energy sector, economics, modeling, risk analysis, and climate change and has experience working for various non-governmental organizations and in numerous research projects on these subjects. In order to improve his abilities and knowledge on renewable energy and electricity grids, he started Master of Science in Natural Resources at North Carolina State University in August 2019. He worked on analyzing the joint probability of the New England bulk electricity grid experiencing wind speeds that exceed turbine cut-out speeds for offshore wind turbines during a cold snap that would result in higher electricity demand and fuel prices. He is planning to continue studying the impacts of climate change and extreme weather events on electricity grids that are increasingly reliant on variable renewable energy.

ACKNOWLEDGMENTS

First of all, I would like to thank my advisor, Dr. Jordan Kern. This study would not have been possible without his valuable guidance, support, and patience. I would also like to thank Dr. Gregory W. Characklis and Dr. Jeremiah Johnson for their contribution and time for this study to be more complete and credible. Moreover, I am grateful to Dr. Jonathan Lamontagne for his contribution that made this study more realistic. Next, I would be happy to acknowledge my family and friends. They were always by my side throughout this study and never hold back their joy and support. Finally, I would like to thank my wife, Ece Ari Akdemir. Her love and support are always endless, which made this study a reality.

This research was supported by the US Department of Energy, Office of Science, as part of research in the MultiSector Dynamics, Earth and Environmental System Modeling Program.

TABLE OF CONTENTS

LIST OF TABLES vii

LIST OF FIGURES viii

Chapter 1. INTRODUCTION 1

Chapter 2. METHODS 6

2.1. Multi-zone UC/ED 6

2.2. Time Series Inputs 8

2.3. Simulating Offshore Wind Power 9

2.4. Experimental Design 13

Chapter 3. RESULTS AND DISCUSSION 16

3.1. Simulation of the 2018 Bomb Cyclone 16

3.2. Longer Simulation under Multiple Wind Integration Scenarios 19

3.3. Limitations 27

Chapter 4. CONCLUSION 28

REFERENCES 30

APPENDICES 36

APPENDIX A. Completing Missing Hourly Wind Speed Data at Project Site 37

APPENDIX B. Downscaling Synthetic Daily to Hourly Wind Speeds at Vineyard Wind Site 38

APPENDIX C. Modeling Electricity Demand 39

APPENDIX D. Modeling Interchange Flows with Adjacent Systems 41

APPENDIX E. UC/ED Model Inputs and Their Usage 42

E.1. Generator Information 42

E.2. Imports and Exports 43

E.3. Solar and Wind Power 44
E.4. Hydropower 45
E.5. Fossil Fuel Prices 45
E.6. Formulation of UC/ED Model 46
E.6.1. Decision Variables 47
E.6.2. Objective Function 47
E.6.3. Constraints 49
APPENDIX F. Validation of the Model 51

LIST OF TABLES

Table 1. Comparison of the results for the January 2018 cyclonic blizzard from ISO-NE study and our UC/ED model 18

Table 2. Electricity price statistics for the five different scenarios in all hours (inclusive) and during cut-out hours for the expanded 69-year simulation..... 21

LIST OF FIGURES

Figure 1 Percentage of different resources in total electrical energy generation in New England (top) (ISO New England, 2020a); impact of 2017-2018 cold snap on the average fuel mix of New England (bottom) (ISO New England, 2020a) 3

Figure 2 System topology of ISO-NE UC/ED model and capacity mix of eight load zones ... 7

Figure 3 (a) Seasonality of daily average dispatchable hydropower; (b) seasonality of daily dispatchable electricity imports (10-day moving average); (c) seasonality of daily average wind speeds (10-day moving average); (d) seasonality of daily electricity demand (10-day moving average) 9

Figure 4 (a) Relationship of demand and temperature in New England; (b) regression of daily peak demand modeling; (c) regression of daily interchange profile modeling; (d) regression of daily wind speed modeling 13

Figure 5 Flowchart of ISO-NE UC/ED model 15

Figure 6 (a) Hourly electricity prices during the cold snap with respect to different scenarios; (b) hourly wind speed fluctuations throughout the cold snap; (c) possible generation from hypothetical 800 MW offshore wind power plant during the cold snap 17

Figure 7 (a) Power curve approximation of MHI Vestas Offshore - V164; (b) distribution of simulated hourly wind speeds (distribution of the wind speed above the cut-out speed is shown in crimson); (c) seasonality of cut-out events; (d) joint distribution of hourly demand and wind speeds 20

Figure 8 (a) Electricity price distribution of 0 MW and 800 MW cases for all simulation hours; (b) electricity price distribution of 0 MW and 4,000 MW cases for all simulation hours; (c) electricity price distribution of 0 MW, 800 MW, and 800 MW No Cut-out cases during cut-out events; (d) electricity price distribution of 0 MW, 4,000 MW, and 4,000 MW No Cut-out cases during cut-out events 23

Figure 9 (a) Seasonality and reason for electricity price spikes in 4,000 MW case; (b) seasonality and magnitude of electricity price spikes in 4,000 MW case. Price spikes are calculated by subtracting prices under 0 MW from prices in other scenarios. Spikes are defined here as differences > $10/MWh. Gray designates spikes due to other reasons (low wind speeds), whereas red shows the spikes due to cut-out events 24

Figure 10 Parallel coordinate plot of all price spike cases in 4,000 MW case with respect to different state variables. The color map is added to show price spike severity for each discrete event. Black triangles in the wind speed column show the wind cut-in speeds and cut-out speeds (below and above which wind power production drops to zero) 26

Figure A1 Comparison of historical and predicted daily day-ahead electricity price 51

Figure A2 Five piecewise linear regression lines and related equations for MHI Vestas Offshore - V164..... 52

Figure A3 (a) Relationship between turbine hub height and frequency of cut-out events; (b) relationship between turbine hub height and annual electricity generation..... 52

Figure A4 (a) Generation mix for 0 MW case during the cold snap; (b) generation mix for 800 MW case during the cold snap; (c) generation mix for 4,000 MW case during the cold snap 53

Figure A5 (a) Change in generation mix in 0 MW case in case of a cut-out event; (b) change in generation mix in 4,000 MW case in case of a cut-out event; (c) change in wind speed and price spike severity during a cut-out event. (Price spike severity is calculated by subtracting 0 MW case prices from 4,000 MW case prices.)..... 54

Figure A6 (a) Seasonality and reason for electricity price spikes in 800 MW case; (b) seasonality and magnitude of electricity price spikes in 800 MW case. Price spikes are calculated by subtracting prices under 0 MW from prices in other scenarios. Spikes are defined here as differences > $10/MWh. Gray designates spikes due to other reasons (low wind speeds), whereas red shows the spikes due to cut-out events..... 55

Figure A7 (a) Impact of demand and hydropower availability on the magnitude of price difference between 4,000 MW and 4,000 MW No Cut-out case during cut-out hours. (Price difference is calculated by subtracting 4,000 MW No Cut-out case prices from 4,000 MW case prices. Color designates the daily hydropower availability.); (b) impact of demand and import availability on the magnitude of price difference between 4,000 MW and 4,000 MW No Cut-out case during cut-out hours. (Price difference is calculated by subtracting 4,000 MW No Cut-out case prices from 4,000 MW case prices. Color designates the daily import availability.)..... 55

Figure A8 (a) Change in generation mix in 0 MW case during wind speeds lower than cut-in speed; (b) change in generation mix in 4,000 MW case during wind speeds lower than cut-in speed; (c) change in wind speed and price spike severity during wind speeds lower than cut-in speed. (Price spike severity is calculated by subtracting 0 MW case prices from 4,000 MW case prices.) 56

Figure A9 (a) Distribution of price differences between 800 MW and 800 MW No Cut-out cases during cut-out events. (Price difference is calculated by subtracting 800 MW No Cut-out case prices from 800 MW case prices); (b) distribution of price differences between 4,000 MW and 4,000 MW No Cut-out cases during cut-out events. (Price difference is calculated by subtracting 4,000 MW No Cut-out case prices from 4,000 MW case prices.) 57

CHAPTER 1. INTRODUCTION

In electric power systems, increased integration of variable renewable energy sources such as wind power will be a crucial factor in satisfying targets for climate change mitigation (Barthelmie & Pryor, 2014; NASEM, 2021; Solaun & Cerdá, 2019; Zhang et al., 2019). Between 2000 and 2019, electricity generation from wind farms grew from 6 billion kilowatt-hours (kWh) to 300 billion kWh in the United States (U.S.), and wind power currently comprises 7.3% of total utility-scale electricity production in the U.S. (EIA, 2020b). Historically, land-based wind power has been the technology of choice, primarily due to lower capital costs. However, planned offshore wind capacity is growing, offering a number of advantages including higher average and less variable wind speeds and proximity to population (demand) centers.

Despite a wide range of improvements that have allowed operators to dampen and absorb the intermittency of land-based and offshore wind power, intermittency still presents significant challenges. In some cases, these challenges are growing in severity due to ever-increasing installed wind capacity (Ren et al., 2018; Wang et al., 2015). Wind speeds fluctuate over multiple time scales (interannual, seasonal, daily, and sub-hourly), leading to variable wind power production (Archer et al., 2017). Downswings in wind power availability typically have to be compensated by dispatchable power sources like natural gas, coal, or oil-fired power plants that have significantly higher marginal costs and emit more CO_2 and other air pollutants (Turconi et al., 2014). In addition, meteorologists (and system operators) have limited capabilities to forecast wind speeds, as the atmospheric system exhibits chaotic behaviors and is nonlinear in nature (Archer et al., 2017; Bessa et al., 2014; Su et al., 2013). In addition to periods of low wind speeds that reduce power production, excessively high wind speeds can also pose a threat to the operation of wind power plants, especially in the offshore environment, which is more prone to extreme weather

events such as tropical and extra-tropical cyclones (Zhang et al., 2019), including severe winter storms. High wind speeds during these types of events can have physically damaging effects on wind turbines themselves, as well as wider impacts on the power grid (Wang et al., 2015). For instance, after wind speeds exceed a certain threshold referred to as a "cut-out" speed (often around 25 meters per second (m/s)), wind turbines stop generating electricity by preventing their rotor shafts from moving (Masters, 2013). When extreme weather events trigger wind speeds above the cut-out speed for many turbines at once, it may lead to large, sudden decreases in electricity generation (Cai et al., 2018; X. Lin et al., 2019). In some systems, the risks associated with a sudden decrease in wind power production may be compounded if extremely high wind speeds occur simultaneously with a spike in demand for electricity or fuel (e.g. increased heating demands). The combined effects would cause a sudden need for generation from more expensive, dispatchable power plants at a time when the grid's supply may already be stressed.

In the U.S., one system that may be particularly susceptible to winter weather storms that simultaneously create extremely high wind speeds and very low temperatures (high fuel and electricity demand) is the Independent System Operator of New England (ISO-NE) system in the Northeastern U.S., which oversees bulk power system operations in six states. Over the last two decades, the generation mix of ISO-NE has been gradually decreasing its reliance on coal and oil and increasing its dependence on natural gas (Figure 1) (Muzhikyan et al., 2019). Installed renewable energy capacity is growing, driven by falling costs and policy mandates. This includes the nation's first major offshore wind farm, a 30 MW facility off the coast of Rhode Island. Another 1,600 MW of offshore wind is expected to be installed in New England by 2027. As of January 2020, 14,200 MW of future wind power are being proposed in the New England region (ISO New England, 2020a).

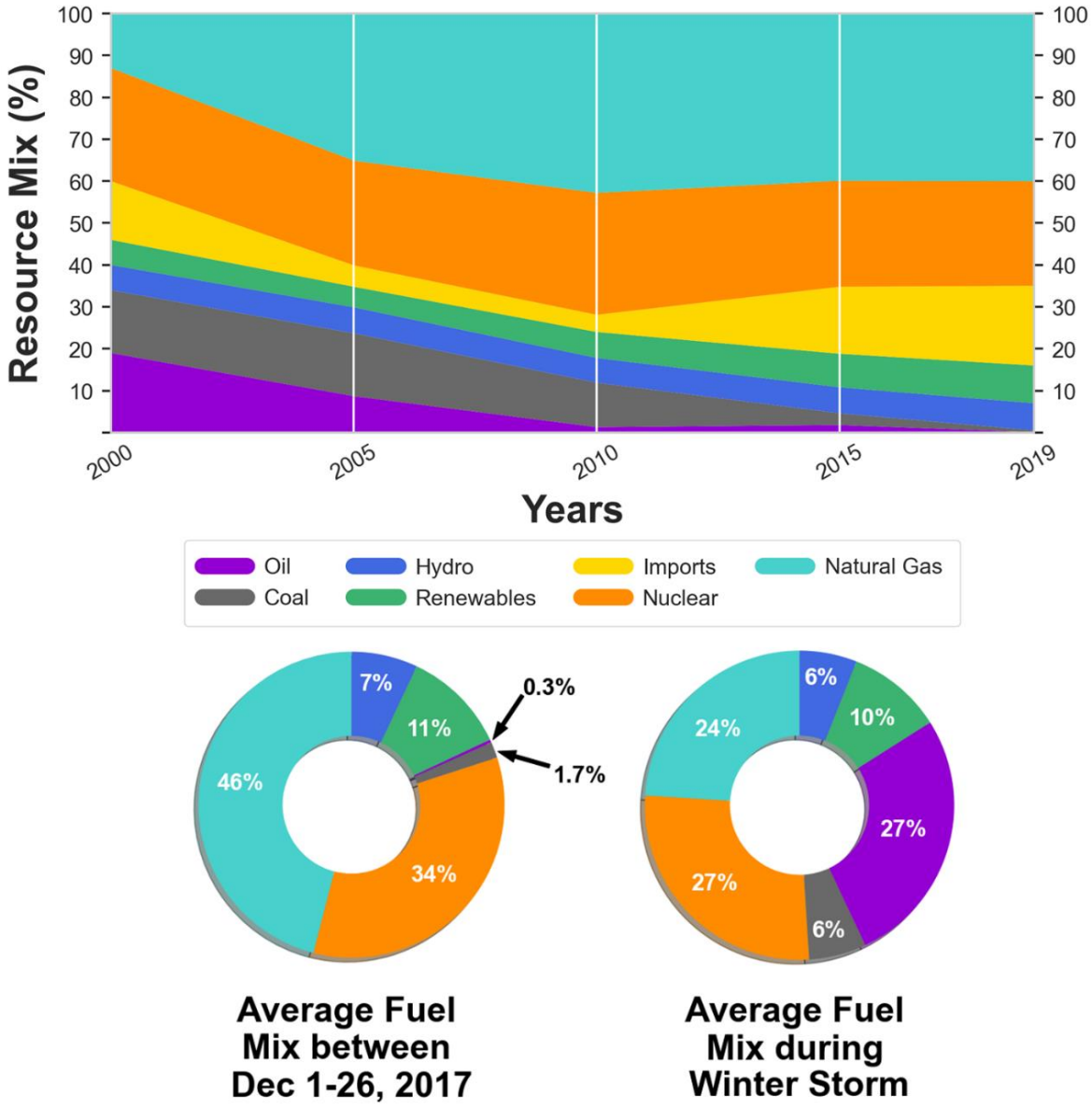

Figure 1: Percentage of different resources in total electrical energy generation in New England (top) (ISO New England, 2020a); impact of 2017-2018 cold snap on the average fuel mix of New England (bottom) (ISO New England, 2020a).

As ISO-NE increases its reliance on offshore wind power, there is some urgency to understand the system's vulnerability to periods of simultaneous, very high wind speeds and low temperatures. For example, between late December of 2017 and early January of 2018, the ISO-NE system experienced a severe winter weather event, an extra-tropical cyclonic blizzard (a "bomb cyclone") that resulted in temperatures plummeting 10°F below normal, which greatly increased

demand for natural gas. Due to increased demand and limited supply (pipeline constraints), natural gas prices increased dramatically, making electricity from natural gas power plants much more expensive and leading to greater reliance on electricity supplied from oil power plants (Figure 1). As a consequence, both market prices and CO_2 emissions increased substantially (ISO Newswire, 2018; Speake et al., 2020). Preliminary research has suggested that the capacity factor of planned/hypothetical offshore wind configurations would have been around 70% over the course of the cold snap. The same study also estimates that the presence of a 400 MW offshore wind plant would have reduced market prices in the ISO-NE day-ahead market by 4-6 USD/MWh (ISO New England, 2018).

However, previous analyses of the benefits of wind power in the ISO-NE system during severe winter weather limit their consideration to a few historical events, and they do not consider the risks of sudden shortfalls in wind power generation due to excessive wind speeds. The use of historical hydrometeorological observations to evaluate critical infrastructure performance has a long history of misrepresenting risks from extreme events (Herman et al., 2016; Lall & Sharma, 1996; Sahin & Sen, 2001). This practice can be particularly problematic when considering risks associated with compound events involving simultaneous extremes in two or more fields (in this case, high wind speeds and low temperatures). The need to more deeply study the risks of extremely high wind/cold snap events on the New England grid also mirrors a general lack of consideration of the hazards posed by extremely high wind speeds in the power systems analysis literature (J. Lin et al., 2012; Wang et al., 2015).

Operations of wind power plants during extreme weather, including high wind cut-out events, and the corresponding impacts to larger electricity grids, have become a critical issue (Cai et al., 2018; X. Lin et al., 2019). Here, we help addressing this current gap in knowledge by

analyzing operations of the ISO-NE system market using a newly developed open-source, multi-zone unit commitment/economic dispatch (UC/ED) model. We analyze the joint probability of the system experiencing wind speeds that exceed turbine cut-out speeds for offshore wind turbines during a cold snap that would result in higher electricity demand and fuel prices. We examine how these events influence market prices, and whether high wind speed cut-out events represent an overlooked vulnerability that could alter longer-term system planning efforts.

CHAPTER 2. METHODS

Our discussion of methods begins with a description of the UC/ED model used to represent the ISO-NE system and its interaction with neighboring systems. We then focus on the meteorological data used and pre-processing steps required, as well as our use of historical meteorological data to estimate power system state variables (i.e. offshore wind power production and zonal electricity demand) for periods outside the recent observed records. A detailed description of our model and all its sub-components can be found in the Appendix E. Validation of the UC/ED model's ability to simulate market price dynamics in the ISO-NE system can be found in Figure A1 of Appendix F.

2.1.Multi-zone UC/ED

For this study, we developed a new, open-source UC/ED model specifically to evaluate hydrometeorological risks in the ISO-NE system. All code and data are freely available via online public repositories. The model accurately reproduces historical price dynamics in the ISO-NE wholesale market, and (when paired with a representation of key stochastic inputs) also offers unique capabilities for exploring the role of hydrometeorological forcings on electricity market outcomes.

The UC/ED model's geographical scope covers the U.S. states of Connecticut, Massachusetts, Rhode Island, Vermont, New Hampshire, and Maine. It is formulated as a mixed-integer linear program using the Pyomo (Python) mathematical optimization package and solved by the commercial solver Gurobi. The model's objective function is to minimize the cost of meeting hourly demand for electricity and operating reserves in the ISO-NE market, subject to constraints on individual generators, the capacity of transmission pathways linking zones, and

others. The model represents the ISO-NE market as a network of eight interconnected load zones (Figure 2), which also exchange electricity with adjacent systems external to the ISO-NE market (these interchanges are modeled statistically). Apart from experimenting with the level of installed offshore wind power capacity, we assume 2018 grid resources, including thermal generators, hydroelectric dams, and high voltage transmission pathways.

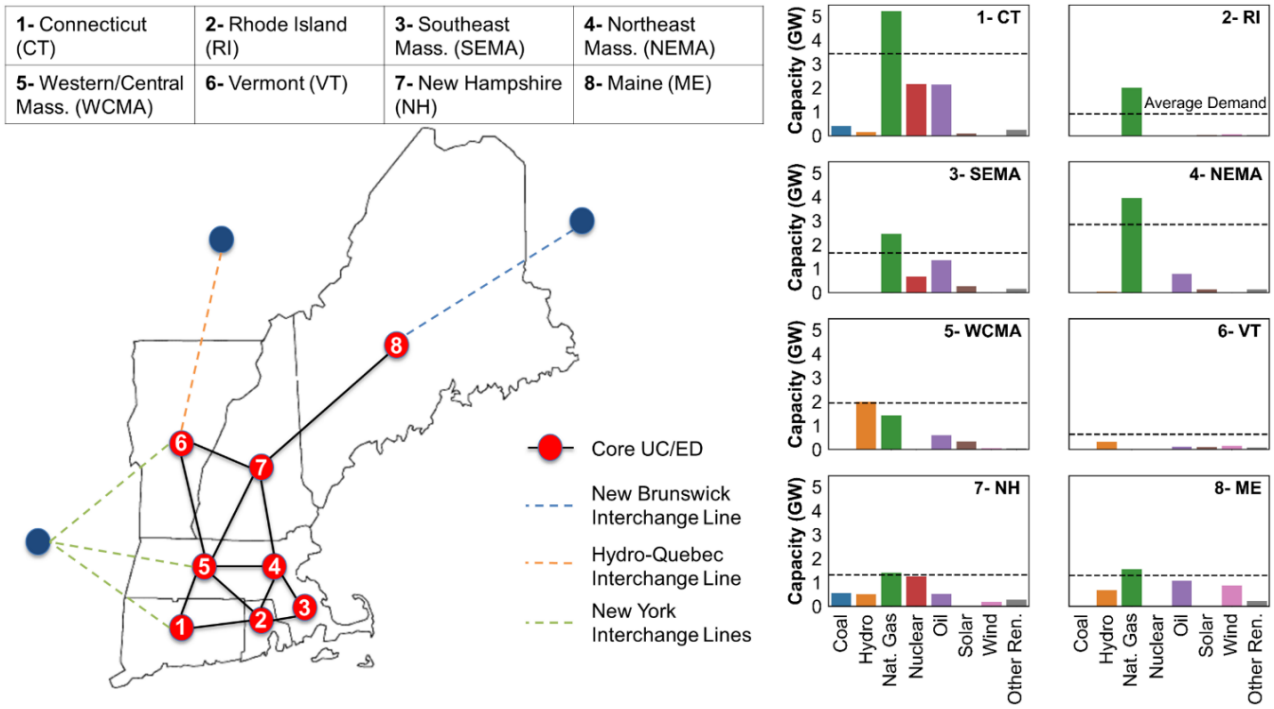

Figure 2: System topology of ISO-NE UC/ED model and capacity mix of eight load zones.

The model iteratively minimizes operational costs associated with meeting electricity demand over a user-defined ("look-out") horizon of 48 hours, while being bound by numerous generator-specific and system-wide constraints. The primary decision variables are binary (on/off) and continuous electricity production variables that control the operations at "dispatchable" generators (coal, natural gas, oil, imports, and hydro). Nuclear, onshore wind, solar and other renewable energy resources are regarded as "must-run" resources due to their low operational cost,

but can also be curtailed if necessary. Model outputs include the least cost generation schedule, identified down to the individual generator level, hourly zonal electricity prices, hourly interchange between zones, and hourly electricity production cost.

2.2.Time Series Inputs

The primary inputs to the UC/ED problem are simulated daily amounts of available hydropower production (Figure 3a), daily electricity imports from adjacent systems (Figure 3b), hourly offshore wind power production (Figure 3c), and hourly time series of electricity demand in each zone of ISO-NE (Figure 3d). Average monthly records of hydropower production reported by the U.S. EIA for each zone are downscaled to constant daily values, which are dispatched optimally by the UC/ED.

Air temperatures and wind speeds are used to simulate daily peak electricity demand via multivariate regression (Figures 4a and 4b), with model residuals represented via vector autoregressive (VAR) models; hourly values are conditionally resampled from the historical record. Interchange data are simulated in a similar statistical manner, using meteorological variables as predictors (Figure 4c). In our statistical demand and interchange models, we use air temperatures and wind speeds at major airports from the National Oceanic and Atmospheric Administration (NOAA) Local Climatological Data (NOAA, 2021). These variables are acquired from seven stations located throughout eight load zones of the ISO-NE market for the period 1949 to 2018 (1959 is omitted due to lack of data). For detailed descriptions of the statistical models used to simulated electricity demand and system interchanges, please see Appendix C and D.

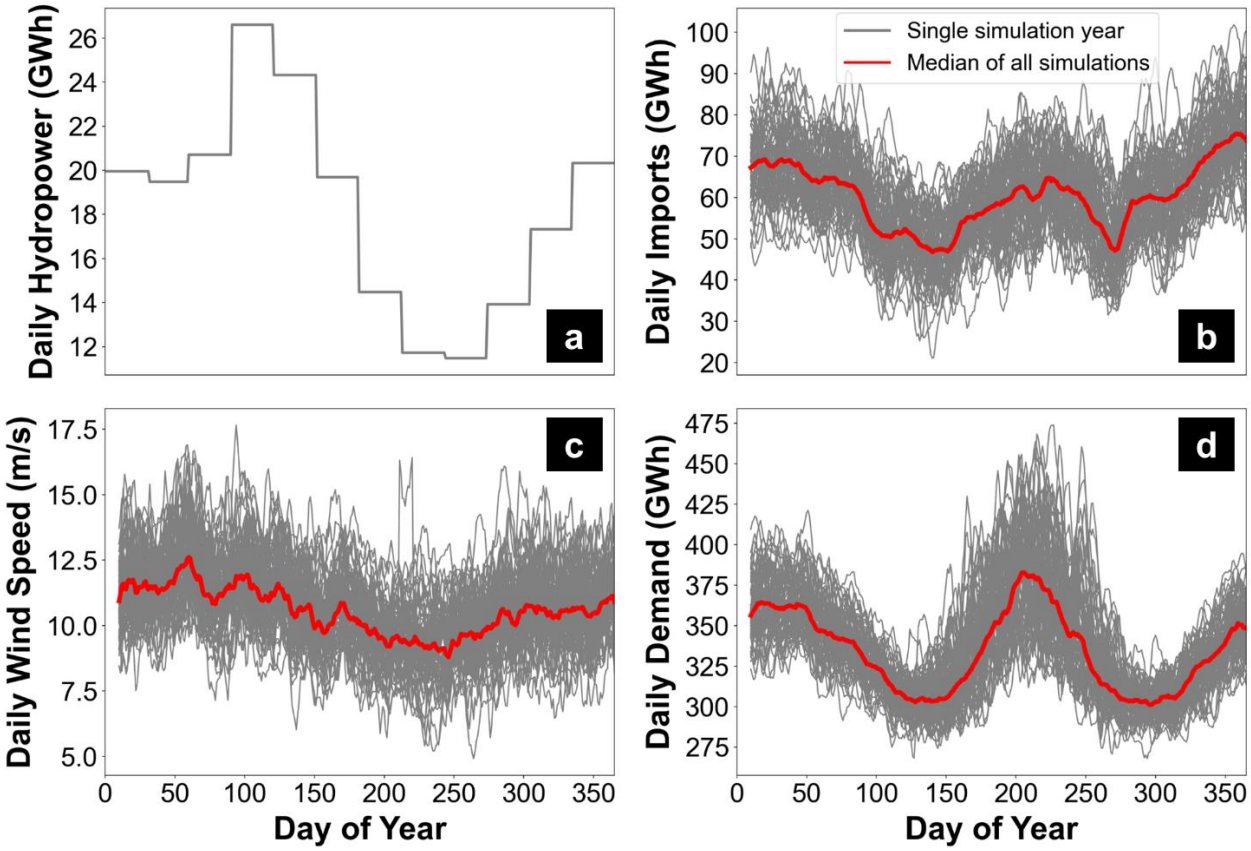

Figure 3: (a) Seasonality of daily average dispatchable hydropower; (b) seasonality of daily dispatchable electricity imports (10-day moving average); (c) seasonality of daily average wind speeds (10-day moving average); (d) seasonality of daily electricity demand (10-day moving average).

2.3.Simulating Offshore Wind Power

We based our analysis of offshore wind power production around the planned construction of a real 800 MW offshore wind project (Vineyard Wind) off the southern coast of Rhode Island and Massachusetts. Observed 10-minute wind speed data at the proposed Vineyard Wind project site are available for a range of different hub heights (ranging from 53 meters to 200 meters) over the period of December 2016 through December 2018. First, these data were resampled into hourly average, daily maximum, and daily average wind speeds, then a limited number of missing data were interpolated (see Appendix A for a detailed description of data interpolation approach).

Only two years of wind speed data are available at the proposed project site. Thus, we used a representative weather station with a much longer observed record (Nantucket Memorial Airport, MA, US) to create an extended wind speed dataset at the Vineyard Wind site. Hourly wind speed data from Nantucket Memorial Airport were gathered for the period 1949-2018 from NOAA Local Climatological Data (NOAA, 2021), and missing data were filled in similar to the approach outlined above. A power law (Gualtieri & Secci, 2012) was used to transform wind speeds recorded at Nantucket Memorial Airport (elevation = 13.7 meters) to wind speeds at each hub height:

$$v_2 = v_1\left(\frac{h_2}{h_1}\right)^{\alpha} \quad (1)$$

Where,

$v_1 =$ Wind speed at elevation h_1 (m/s)

$v_2 =$ Wind speed at elevation h_2 (m/s)

$\alpha =$ Wind shear exponent

Observed wind speed data at the project site contains hub heights of 53, 60, 80, 90, 100, 110, 120, 140, 160, 180, and 200 meters. Between 13.7 meters and 53 meters, wind shear (α) is calculated by the formula below (Gualtieri & Secci, 2011):

$$\alpha = \left(\frac{z_0}{h_1}\right)^{0.2}[1 - 0.55\log(v_1)] \quad (2)$$

Where,

$z_0 =$ Roughness length (m)

Roughness length is assumed as 0.03 m, which is selected with respect to geographic characteristics of Nantucket Island by using WMO Guide (World Meteorological Organization, 2008). At hub heights above 53 meters, wind shears are calculated by comparing time-series data from the project site. In this study, wind turbine hub height is selected as 110 m to be as close as possible to Vineyard Wind project's approximate hub height of 105 m (MHI Vestas Offshore Wind, 2017). Thus, the formula below is used to initially calculate wind shear for every hour (Gualtieri & Secci, 2011):

$$\alpha = \frac{\ln\left(\frac{v_2}{v_1}\right)}{\ln\left(\frac{h_2}{h_1}\right)} \tag{3}$$

Wind shear values at a hub height of 110 m for every hour between 2016 and 2018 are then converted to an average 8760-hour profile for the calendar year, which we apply across the full 1949-2016 Nantucket dataset when transforming it from a height of 13.7 m to 110 m.

To extend the Vineyard wind data, we train a linear regression model on daily wind speeds at the two sites (Nantucket and Vineyard Wind) for the period 2016-2018 (Figure 4d). Residuals from the fitted regression do not exhibit statistically significant levels of autocorrelation. In order to generate synthetic residuals, we fit the residuals to Weibull and Burr distributions, and randomly sample values for the period 1949-2016. These synthetic residuals are then added to regression predictions for the same period, giving us an extended record of daily wind speeds at the Vineyard Wind site for the period 1949-2016; this is then added to observed values at the Vineyard Wind site for 2016-2018. Downscaled hourly wind speeds are then created through a conditional resampling approach (see Appendix B for detailed description).

We then translate hourly wind speeds to hourly values of wind power production. The power curve of the specific turbine proposed for the project (9.5 MW MHI Vestas Offshore - V164) is broken into five piecewise linear segments (see Figure A2). Cut-in and cut-out speeds of this turbine are 3.5 and 25 m/s, respectively (The Wind Power, 2021). In other words, wind power output drops to zero when wind speeds are below 3.5 m/s or above 25 m/s. Taking cut-in and cut-out wind speeds into consideration, wind power production is simulated between 1949-2018 by utilizing a linear regression approach. Note that we do not account for any potential differences in wind speeds among turbines within the array. Nor do we fully explore the effects of alternative hub heights, though we did perform a sensitivity analysis to understand potential tradeoffs between average generation and cut-out frequency (see Figure A3). As expected, average electricity generation and the frequency of cut-out events both increase as hub height increases, since higher hub heights experience higher speeds. In this sense, apart from growing capital costs, there is an unavoidable tradeoff between electricity generation and the number of cut-out events when hub height of the wind turbines increases.

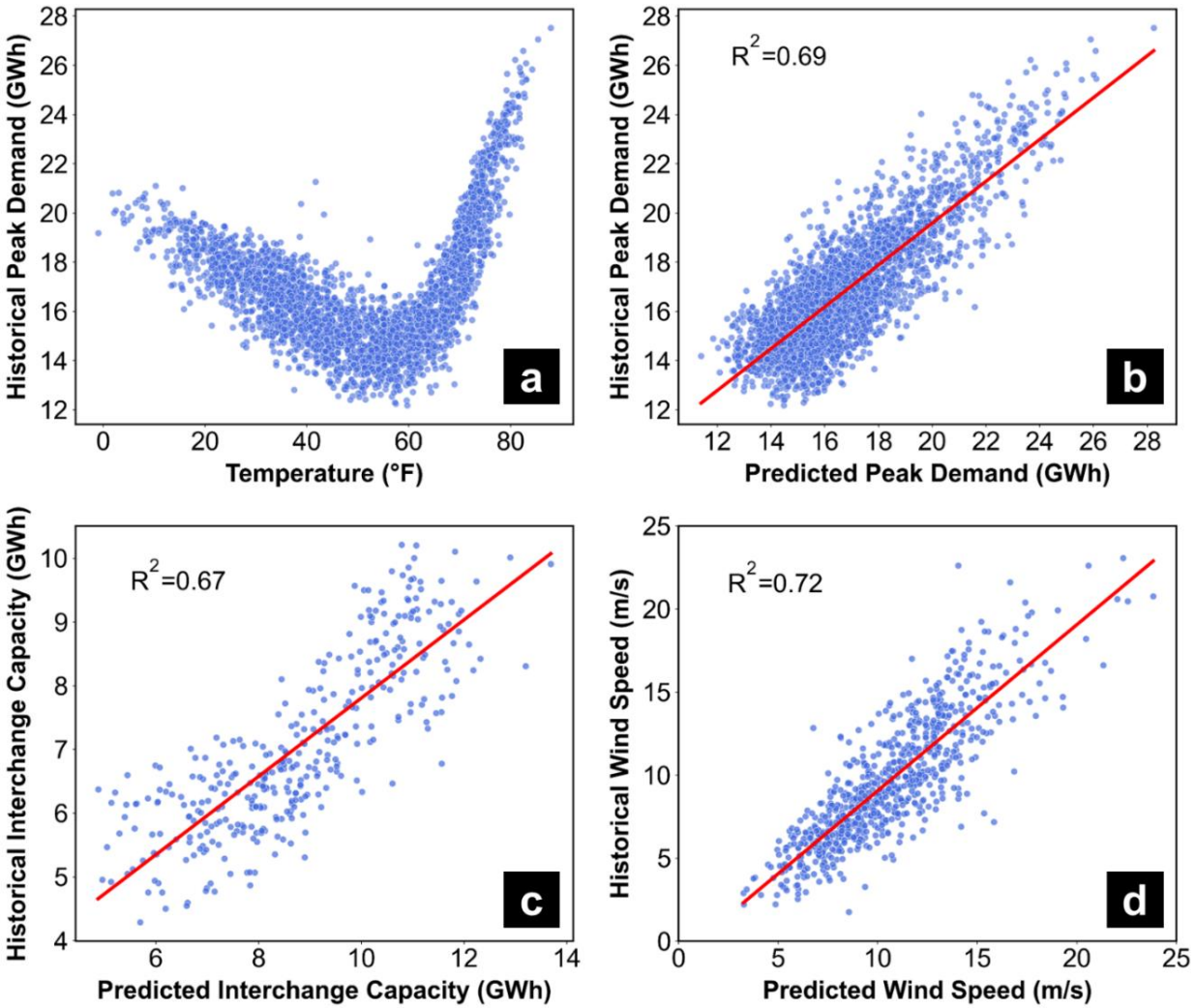

Figure 4: (a) Relationship of demand and temperature in New England; (b) regression of daily peak demand modeling; (c) regression of daily interchange profile modeling; (d) regression of daily wind speed modeling.

2.4.Experimental Design

We use our model first to reproduce outcomes in the ISO-NE system during the cyclonic blizzard that occurred between late December of 2017 and early January of 2018 (Figure 1). Throughout this period, electricity demand and natural gas prices increased substantially as a result of extremely low temperatures. Consequently, dependence on oil power plants increased, which in turn causes a sudden increase in wholesale electricity prices as well as emissions. Considerable attention has already been paid to how this particular event impacted the ISO-NE system (i.e. its

impact on demand for electricity and fuel, and subsequent increases in market prices) (ISO New England, 2018). We validate the ability of our model to capture market price dynamics and resource usage reported by ISO-NE. Then we provide estimates of the potential impacts of hypothetical offshore wind power plants on production costs, emissions, fossil fuel use, and locational marginal prices (LMPs) during this winter weather event, and compare our findings to results from a high-level analysis performed by ISO-NE. We explore the response of the ISO-NE system during the 2017-2018 winter weather event under three different offshore wind power integration scenarios: 0 MW (historical system operations), 800 MW, and 4,000 MW. Under each scenario, historical natural gas and oil prices are assumed.

In the second part of our analysis, the behavior of the ISO-NE system is simulated over a much longer time period (1949-2018) using our extended hydrometeorological dataset, in order to probabilistically estimate risks associated with winter weather cut-out events. We explore system behavior under five different offshore wind power integration scenarios: 0 MW, 800 MW, and 4,000 MW; in addition, for the 800 MW and 4,000 MW wind power scenarios, we consider two more scenarios in which wind speeds above 25 m/s do not trigger cut-out events. The "No Cut-out" scenarios are used to control for the specific impacts of excessive wind speeds on system outcomes (e.g. wholesale prices). For this 69-year simulation, 365-day oil and natural gas price profiles are created from recently observed data and applied uniformly across each simulation year. Detailed descriptions of the generation of fuel prices can be found in Appendix E.5. Our overall modeling approach and experimental design are summarized in Figure 5.

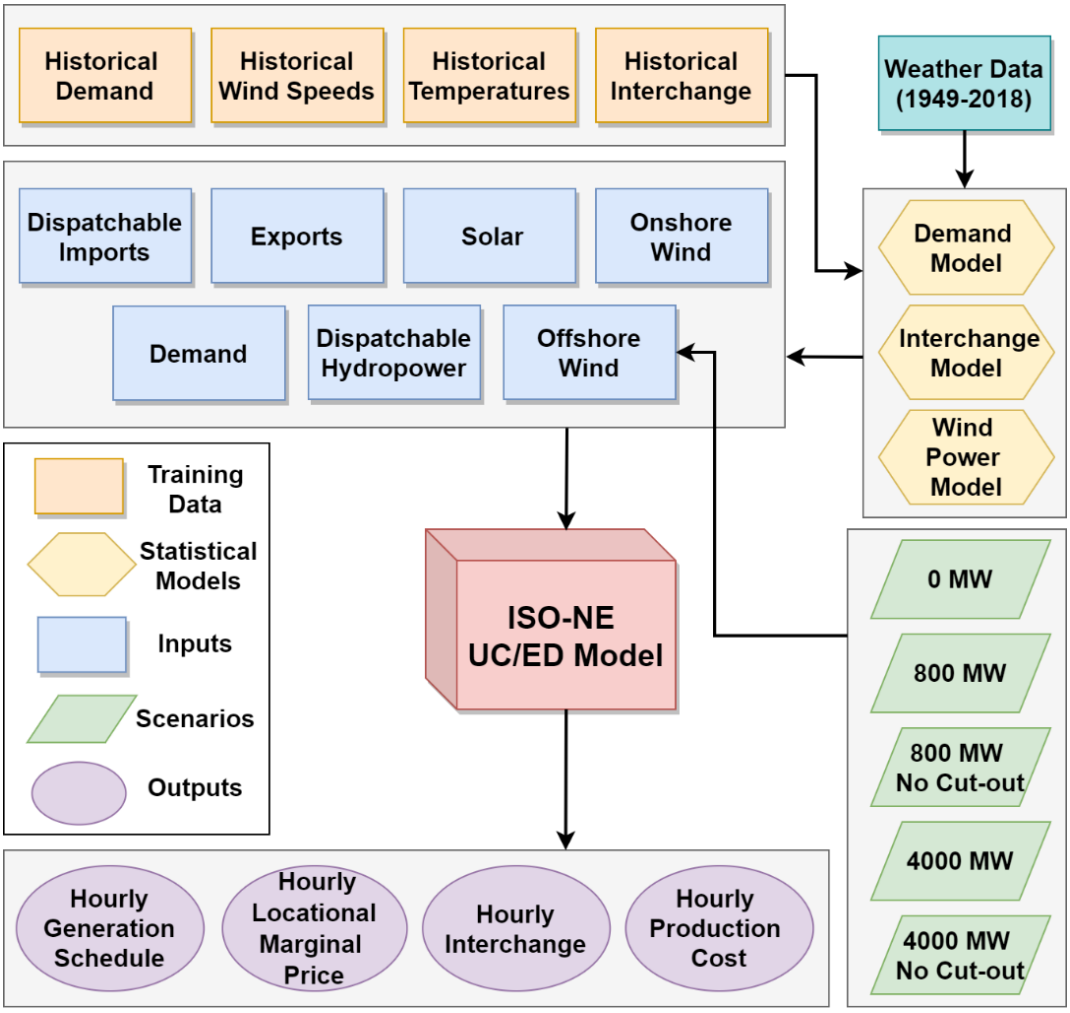

Figure 5: Flowchart of ISO-NE UC/ED model.

CHAPTER 3. RESULTS AND DISCUSSION

Discussion of the results is organized in two main sections. First, we explore outcomes from the simulation of the 2017-2018 cyclonic blizzard that impacted the ISO-NE system. Second, probabilistic results from the 69-year simulation under five different wind power scenarios are explored.

3.1.Simulation of the 2018 Bomb Cyclone

Our results confirm that the 2017-2018 bomb cyclone significantly disrupted the ISO-NE market (Figure 6). Without any wind power capacity present (0 MW wind case), hourly electricity prices rise in late December to around $150/MWh (driven by increased fuel prices in expectation of the storm) and then to over $340/MWh during the height of the event (January 5). Figure 6 shows that the presence of hypothetical offshore wind generation in the system lessens the severity of these price spikes, even though wind power is temporarily lost due to a cut-out event on late January 4 (Figure 6a and 6b). Note that under a 4,000 MW case, this sudden loss of wind generation due to a cut-out event causes a price increase of +$20/MWh from one hour to the next. However, compared to the relative reduction in market prices caused by the steady presence of 4,000 MW of offshore wind energy the next day on January 5, the price increase due to the cut-out event appears negligible. Although wind power output is variable along the cold snap, we estimate the capacity factor of a hypothetical 800 MW offshore wind power would have been 65.63% (Figure 6c).

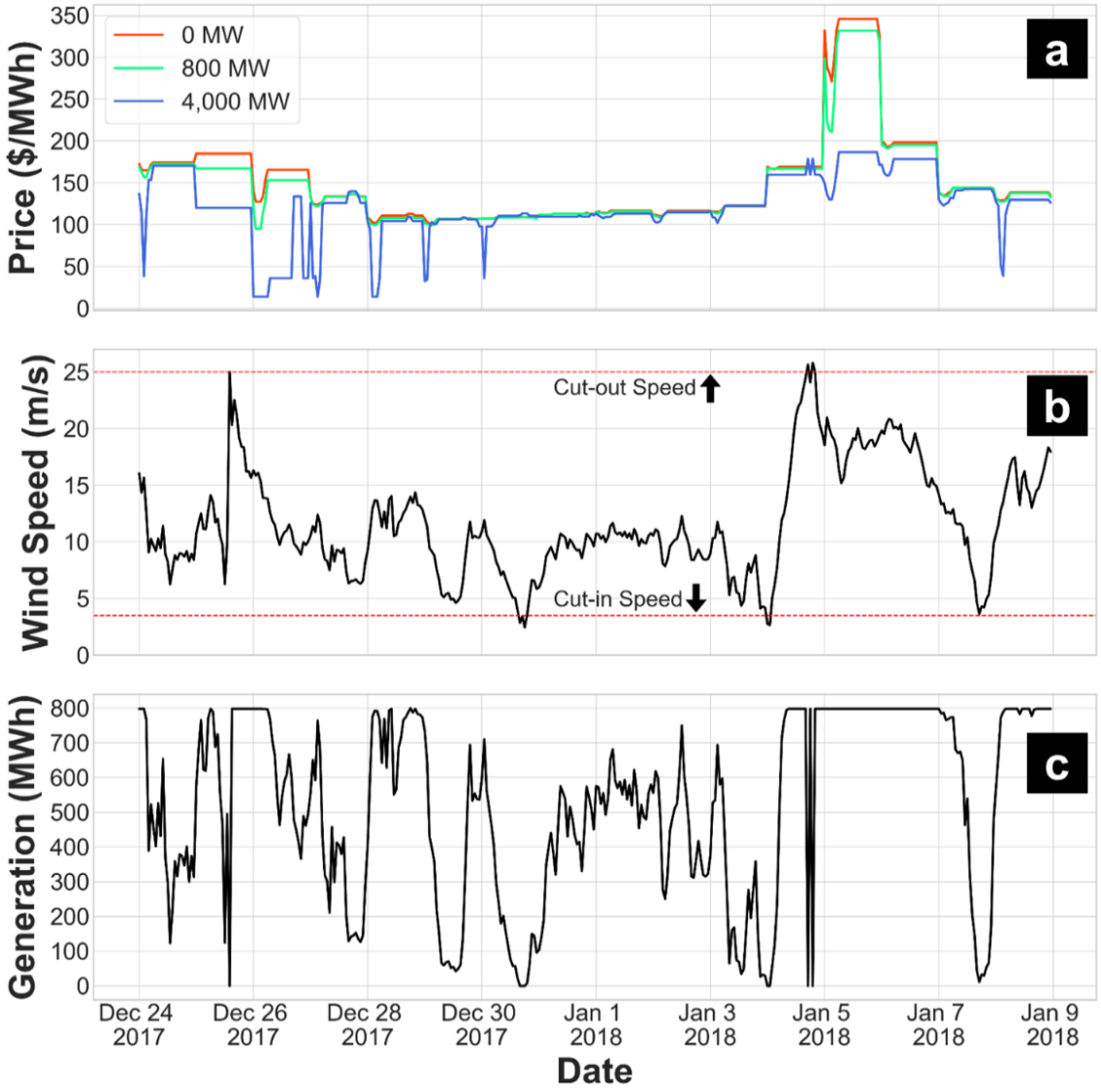

Figure 6: (a) Hourly electricity prices during the cold snap with respect to different scenarios; (b) hourly wind speed fluctuations throughout the cold snap; (c) possible generation from hypothetical 800 MW offshore wind power plant during the cold snap.

Offshore wind power, having smaller marginal generation costs, would have displaced electricity generation from oil and natural gas power plants in the ISO-NE market. During the cold snap, an 800 MW offshore wind power could have displaced 49.8 GWh and 151.1 GWh of oil and natural gas generation (and associated greenhouse gas emissions), respectively. Figure A4 provides a detailed look at daily and hourly generation mix dynamics simulated by our model for both levels of installed wind power capacity (800 MW and 4,000 MW).

Table 1 compares the estimated effects of 800 MW of offshore wind power on market prices and resource usage during the 2017-2018 bomb cyclone from our analysis alongside results of a study conducted by ISO-NE (ISO New England, 2018). Our findings are similar, with differences likely explained by our approach for wind modeling (which estimates a lower capacity factor), our use of publically available fuel price information (coarser in spatial and temporal resolution than what ISO-NE would use), and our estimates of some generator specific operating parameters. ISO-NE estimates a relative decrease in market prices of $6-8/MWh with 800 MW in place, while our model predicts a relative decrease of $4.45/MWh. With 4,000 MW of offshore wind in place, our modeling suggests a significantly larger relative price drop of $28.81/MWh over the roughly 2-week period from December 24, 2017 to January 9, 2018. Note in particular that during the height of the bomb cyclone on January 5, the presence of 4,000 MW would have reduced prices by as much as $150/MWh. Thus, for this historical event, there is evidence that the price (and emission) reduction benefits of greater offshore wind power capacity outweigh the risks associated with sudden wind turbine cut-out events from excessive wind speeds.

Table 1: Comparison of the results for the January 2018 cyclonic blizzard from ISO-NE study and our UC/ED model.

Performance Parameter	**ISO-NE Study (800 MW)**	**UC/ED Model (800 MW)**	**UC/ED Model (4,000 MW)**
Offshore Wind Power Generation (MWh)	215,569	201,103	1,005,517
Average Capacity Factor Over Cold Snap (%)	70	65.63	65.63
Displaced Natural Gas Generation (MWh)	114,600	151,212	699,913
Displaced Oil Generation (MWh)	56,000	49,866	282,807
Average Day-Ahead Electricity Price Change ($/MWh)	-8 to -6	-4.45	-28.81

3.2.Longer Simulation under Multiple Wind Integration Scenarios

In order to further explore the role of wind turbine cut-out events on the ISO-NE market, we simulate system behavior over the period 1949-2018 (1959 is omitted due to lack of data, for a total of 69 years or 604,440 operational hours) under five different offshore wind integration scenarios (see green scenarios in Figure 5). The use of this expanded dataset greatly enhances our ability to characterize probabilistically the impacts of wind speed cut-out events on the ISO-NE system. The specific wind turbine proposed for Vineyard Wind project has a cut-in speed of 3.5 m/s and a cut-out speed of 25 m/s (Figure 7a). Going below the cut-in speed and above the cut-out speed causes wind power production to fall to zero. Over the 69-year simulation period, hourly wind speeds at a hub height of 110 m mostly fluctuate between 7-14 m/s, with an average speed of 10.7 m/s; the full range of wind speeds simulated ranges between 0.1 m/s and 85.6 m/s. Over the same period, the probability of experiencing wind speeds below the cut-in threshold in a given hour is 3.14%, whereas the probability of experiencing a cut-out event is 0.21% (Figure 7b).

When the seasonality of cut-out events from excessive wind speeds is examined, we see that most occur during winter, early spring, and late fall seasons (Figure 7c). This outcome is somewhat expected given seasonal wind speed trends in the New England region (see Figure 3c). The seasonality of cut-out events could amplify the probability of ISO-NE facing sudden wind turbine losses from excessive wind speeds during a period in which severe winter weather is simultaneously causing high electricity demand and natural gas prices. To assess this risk visually, we inspect the joint distribution of wind speeds and electricity demand for the ISO-NE system (Figure 7d). Despite the fact that most cases are centered around 10 m/s wind speed and 14,000 MWh electricity demand, there is a considerable chance of ISO-NE experiencing cut-out events during high demand periods. Note as well that we can clearly see the occurrence of rare, but

plausible events in which electricity demand and wind speeds increase to extreme levels (dashed box in Figure 7d). A key focus of our analysis is whether these events pose risks to the ISO-NE system that outweigh the operational advantages of added wind power capacity.

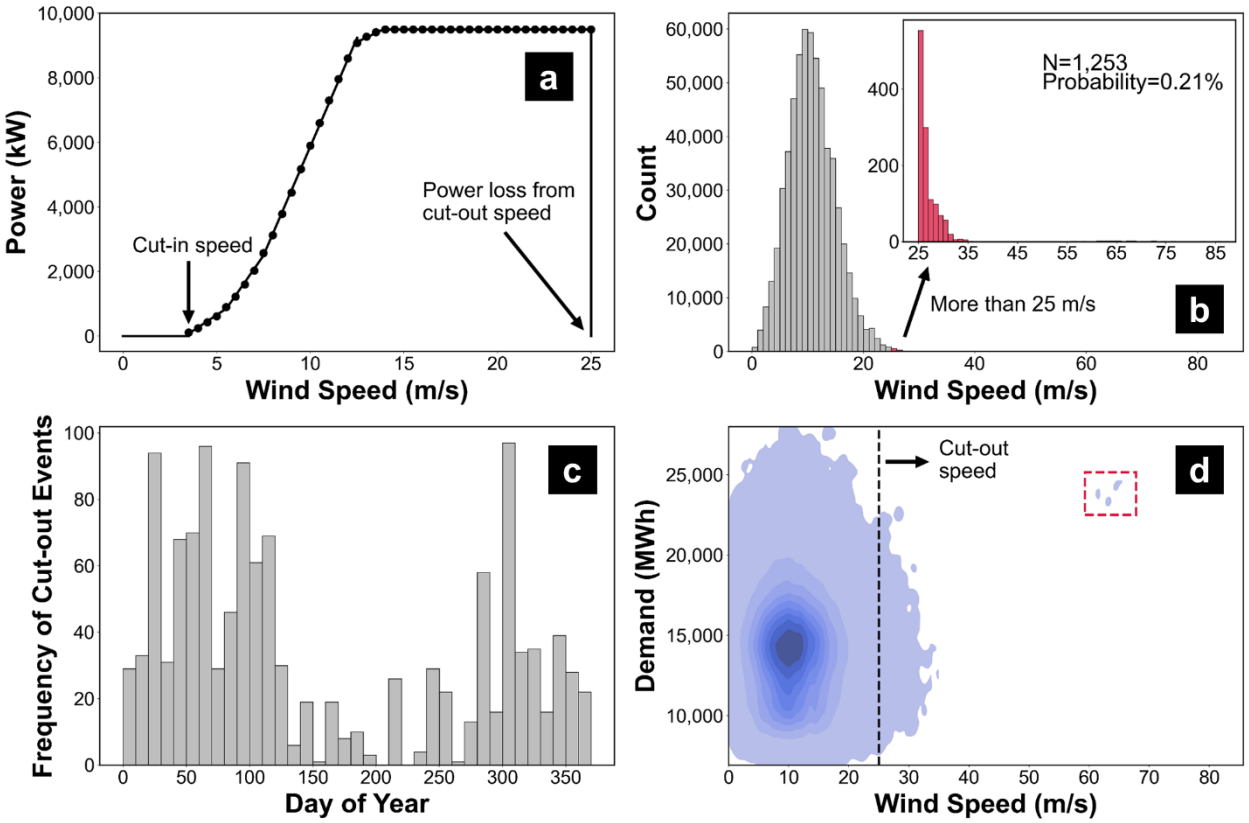

Figure 7: (a) Power curve approximation of MHI Vestas Offshore - V164; (b) distribution of simulated hourly wind speeds (distribution of the wind speed above the cut-out speed is shown in crimson); (c) seasonality of cut-out events; (d) joint distribution of hourly demand and wind speeds.

Over the expanded 69-year simulation period, we find that integrating offshore wind power to the ISO-NE bulk electricity system leads to a significant reduction in average wholesale electricity prices, and the extent of the relative price drop is most pronounced in the 4,000 MW case (see Table 2, and Figures 8a and 8b). Average electricity prices throughout the simulation period are $35.15/MWh in the 0 MW wind power case. On average, 800 MW and 4,000 MW of offshore wind power capacity lead to decreases in hourly electricity prices of $0.20/MWh and

$2.1/MWh, respectively. However, Table 2 also provides evidence that adding more offshore wind power to the ISO-NE bulk power grid could increase the maximum prices experienced, either due to price shocks from cut-out events, from periods of extremely low wind speeds, or both.

In order to help identify the cause of these high maximum prices, we also explore two additional scenarios in which 800 MW and 4,000 MW of offshore wind power are installed, but wind speeds above 25 m/s do not result in losses of wind generation (i.e. "no cut-out" scenarios in Table 2 and Figure 8). In other words, even after wind speeds go above the cut-out speed, wind power output is not disrupted, and the offshore turbines continue to operate at their maximum rated power.

Table 2: Electricity price statistics for the five different scenarios in all hours (inclusive) and during cut-out hours for the expanded 69-year simulation.

	Electricity Price for All Hours ($/MWh)			**Electricity Price for Cut-out Hours ($/MWh)**		
Scenario	**Minimum**	**Average**	**Maximum**	**Minimum**	**Average**	**Maximum**
0 MW	14.02	35.15	218.21	22.59	38.54	114.45
800 MW	10.37	34.95	296.58	22.76	38.62	115.99
800 MW No Cut-out	10.37	34.95	286.48	21.18	37.83	114.41
4,000 MW	10.37	33.05	219.62	10.37	39.43	176.56
4,000 MW No Cut-out	10.37	33.05	219.62	10.37	33.95	107.45

Table 2 shows that, across all hours (left-most columns), the no cut-out scenarios exhibit very similar prices to their counterparts (i.e. comparing 800 MW to 800 MW no cut-out, and comparing 4,000 MW to 4,000 MW no cut-out). However, the specific effects of cut-out events become more apparent if we separate-out and analyze hours in which excessive wind speeds occur (right-most columns of Table 2, Figures 8c and 8d). During cut-out events, dispatchable generators

such as thermal power plants must quickly compensate for a sudden loss of wind power, either by starting plants that are offline, ramping-up production at plants that are online, or both. Consequently, wholesale electricity prices increase and (frequently) surpass prices that would occur with no wind power installed (the 0 MW case) (see Figures 8c and 8d, and Figure A5).

We see that during cut-out hours, the average impact of a sudden loss of 800 MW of wind generation is a price increase of +$0.08/MWh relative to the 0 MW case (whereas prices would be -$0.71/MWh lower under the 800 MW case if no cut-out had occurred). Under the 4000 MW case, we see that cut-out events cause an average price increase of +$0.89/MWh relative to the 0 MW case, whereas prices would be -$4.59 lower if no cut-out had occurred). The maximum observed effects from cut-out events are +$1.54/MWh with 800 MW of wind installed, and +$62.11 with 4,000 MW installed. Yet, we also observe that the maximum electricity price during cut-out events is $115.99 $/MWh under 800 MW of installed wind power and $176.56/MWh with 4,000 MW installed. In both cases, the maximum price observed in all hours is well above these levels. This suggests that wind cut-out events from excessive wind speeds are not responsible for the highest prices observed over the 69-year simulation period—rather, those prices are likely to be driven by a different vulnerability associated with large scale wind integration, e.g. periods of very low wind speeds and/or high variability.

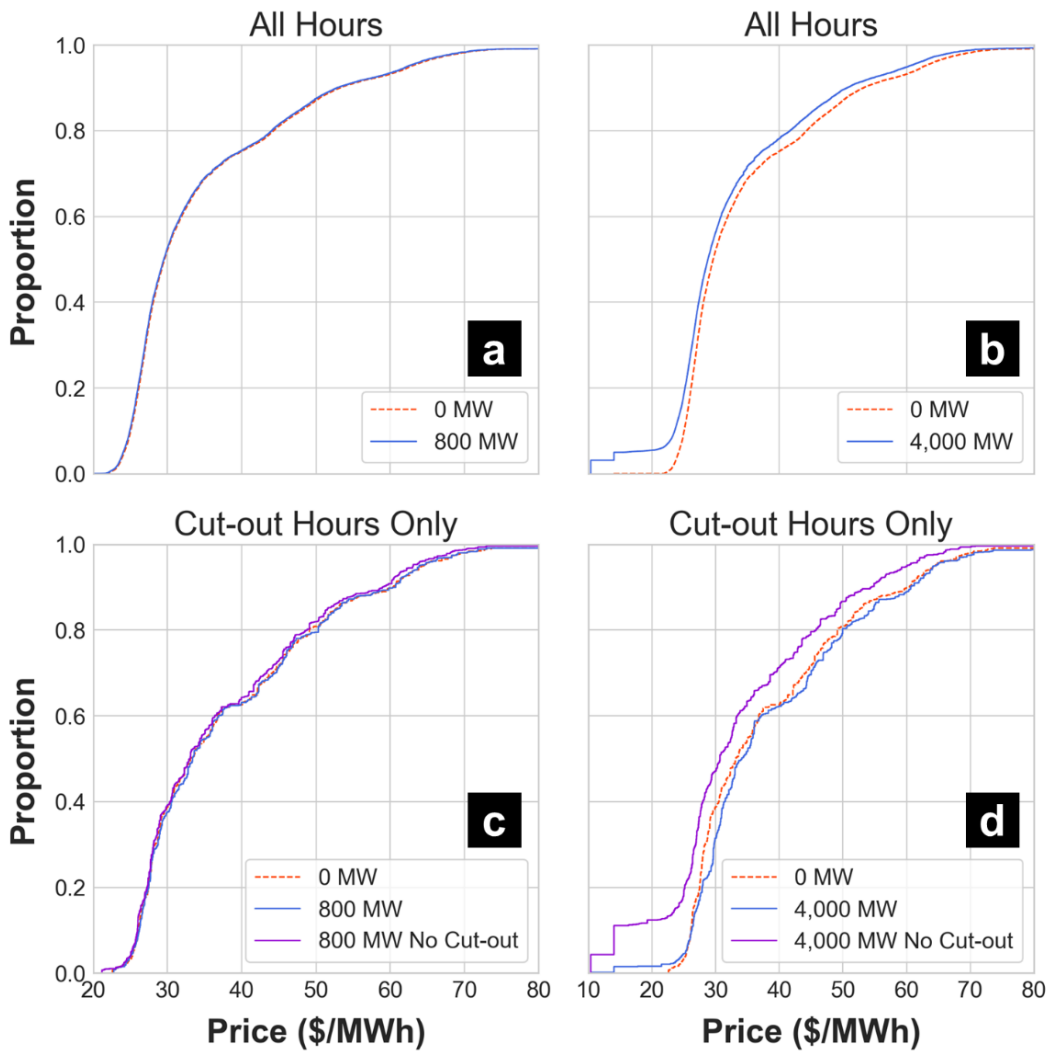

Figure 8: (a) Electricity price distribution of 0 MW and 800 MW cases for all simulation hours; (b) electricity price distribution of 0 MW and 4,000 MW cases for all simulation hours; (c) electricity price distribution of 0 MW, 800 MW, and 800 MW No Cut-out cases during cut-out events; (d) electricity price distribution of 0 MW, 4,000 MW, and 4,000 MW No Cut-out cases during cut-out events.

In order to disentangle the separate effects of multiple, wind speed related phenomena on the operations of the ISO-NE market, we quantify the share of electricity price spikes observed under wind power scenarios due to cut-out events vs. those due to other reasons (low wind speeds). Here, we define a price spike as any hourly difference of more than $10/MWh observed between the 0 MW scenario and the wind power scenarios. We find that cut-out events are responsible for 0% of price spikes observed in 800 MW case (see Figure A6) and 1.38% of the price spike events

in 4,000 MW cases (Figure 9a). Since wind power presence is considerably low in 800 MW cases, cut-out events do not cause a price spike of more than $10/MWh. When a lower price spike threshold (<$10/MWh) is assumed, cut-out induced price spikes are also present in 800 MW case. In addition, we find that cut-out induced price spikes are scattered throughout the year, rather than being aggregated in the winter (when most physical cut-out events occur (see Figure 7c)). Figure 9a shows that most price spikes caused by wind integration are associated with low wind speeds in late summer.

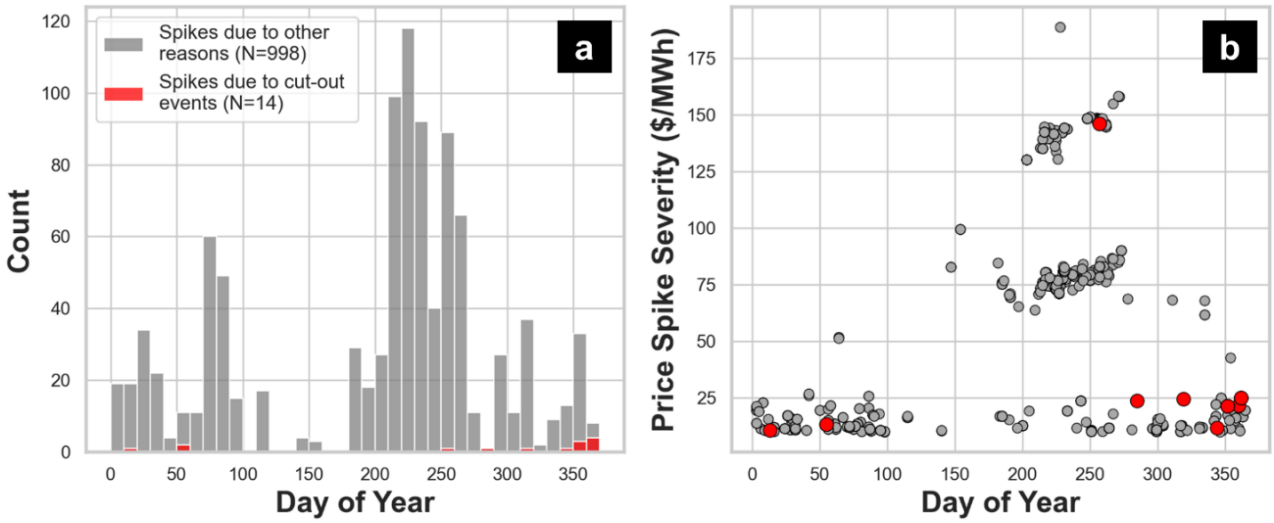

Figure 9: (a) Seasonality and reason for electricity price spikes in 4,000 MW case; (b) seasonality and magnitude of electricity price spikes in 4,000 MW case. Price spikes are calculated by subtracting prices under 0 MW from prices in other scenarios. Spikes are defined here as differences > $10/MWh. Gray designates spikes due to other reasons (low wind speeds), whereas red shows the spikes due to cut-out events.

Figure 9b shows every wind-caused price spike observed over the 69-year simulation period under the 4,000 MW installed wind scenario, identified by its timing and magnitude. Each spike is also colored according to whether it is associated with a high wind speed cut-out event (red) or other reasons (low wind speeds, gray). Note that the most damaging price spike from cut-out events occurs during the late summer, even though most cut-out events occur during winter

when wind speeds are higher. Figure 9b also shows that price spikes due to low wind speeds are likewise more severe during summer. Similar trends are also observed under the 800 MW case (see Figure A6).

Hours with observed price spikes are further evaluated to identify, in each case, the precise combination of underlying forces causing them to occur. Figure 10 shows all hours in the 4,000 MW wind power scenario with market prices $10/MWh or higher than prices in the same hours under 0 MW wind scenario. Each individual line in the parallel coordinate plot shows data for a single hour, and we are able to track how the magnitude of any given price spike (color, first column) corresponds to values in the same hour for electricity demand, wind speeds, natural gas prices, and day of the year. We find that price spikes associated with the adoption of 4,000 MW of wind power concentrate in three bands of severity. The highest severity band (colored dark red) is generally associated with higher electricity demand and low wind speeds (in some cases, lower than the cut-in wind speed) during the summer. This trend is internally consistent with the seasonality of hydrometeorological, and power system state variables observed in the ISO-NE system. In the Northeastern part of the US, including the New England region, electricity demand is highest during summer due to increased usage of air conditioning (Figure 3d), and daily average wind speeds are lower (Figure 3c). Households heated with electricity comprise 16% of all homes (EIA, 2018), with most homes using natural gas and heating oil. In addition, daily dispatchable imports from other regions and hydropower availability are lower than average in summer (see Figures 3a and 3b). The severity of the price spike depends on several factors including the duration of the wind power loss event, demand during and after the incident and, (weakly) import and hydropower availability in the system (see Figure A7). Price spikes due to cut-out events are shown in Figure 10 above the 25 m/s mark in the wind speed column (the 25 m/s threshold is

indicated by a black triangle); these tend to be associated with lower electricity demand during the early spring, late fall, and winter, and are less severe overall. Again, these results suggest that the main vulnerability of a future ISO-NE bulk power grid that is significantly more reliant on wind power will be low wind speeds and sudden drops in wind speeds during high demand hours in the summer (Figure A8). Cut-out events caused by extremely high wind speeds during winter storms likely represent a much lower risk.

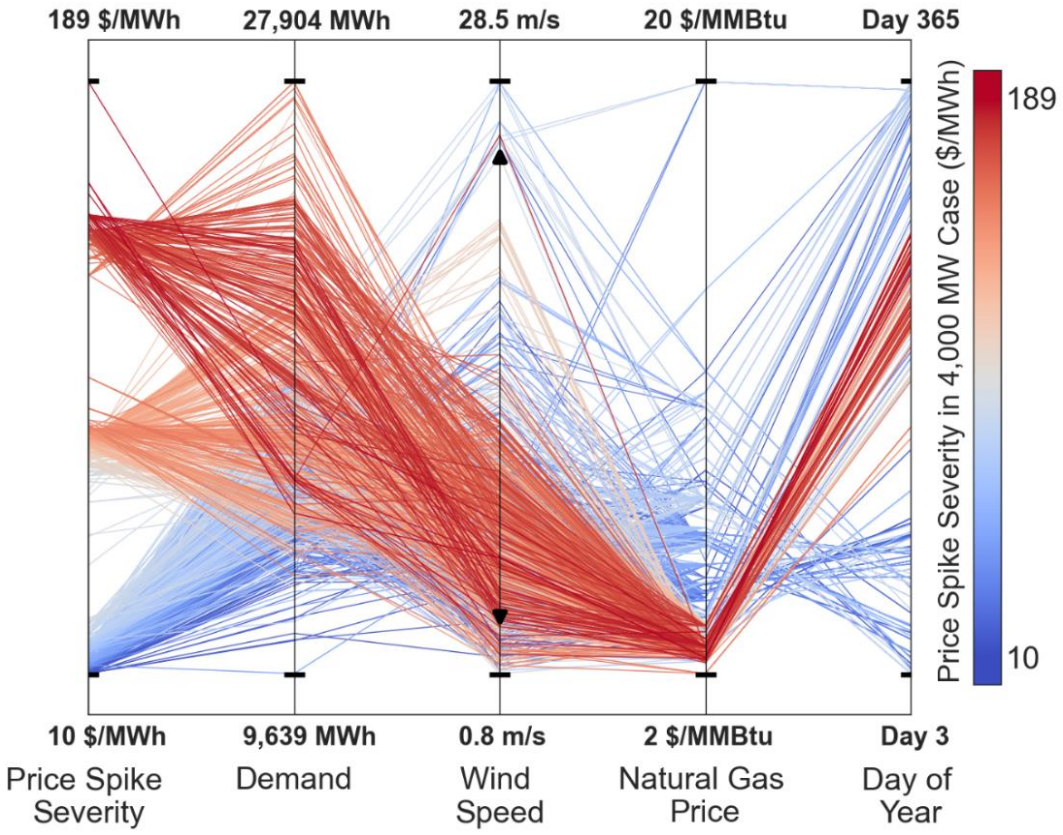

Figure 10: Parallel coordinate plot of all price spike cases in 4,000 MW case with respect to different state variables. The color map is added to show price spike severity for each discrete event. Black triangles in the wind speed column show the wind cut-in speeds and cut-out speeds (below and above which wind power production drops to zero).

3.3.Limitations

There are some limitations of this study. This model focuses on the bulk electricity grid of ISO-NE with just eight nodes, which reduces our ability to capture higher resolution performance issues such as transmission congestion. In addition, lack of access to long-term fuel prices and using a simplified approach to hydropower resources in the region have an impact on the model's representation of the system. Moreover, due to the model's operating horizon approach and other assumptions on the pricing of resources, there are some rare cases where electricity prices in normal cases are less than no cut-out cases during cut-out events (Figure A9). This could arise from our representation of the system as a day-ahead market with perfect foresight (meaning the system operator can in fact anticipate and plan for cut-out events within a 48-hour scheduling horizon). This may also reduce the severity of some of the observed impacts of cut-out events in our study. In reality, successfully managing cut-out events would rely on system operators' ability to allocate and use sufficient supplies of operating reserves. Lastly, there is only one turbine hub height is considered in this study. In the future, other hub heights can also be used in the model to check the sensitivity of the price impacts of cut-out events.

CHAPTER 4. CONCLUSION

In this study, a unit commitment/economic dispatch (UC/ED) model of the ISO-NE bulk electricity grid is developed and used to simulate power system operations during the cold snap that occurred in 2017-2018 winter, and over a longer period (1949-2018). Our aim was to explore the system's vulnerability to sudden losses of wind power due to excessive wind speeds, especially during severe winter weather events. The model, which is freely available via online repositories, uses a zonal approach to represent power systems operations in New England, and it is able to capture 71% of the daily price variability in ISO-NE market.

The results of this study suggest that despite higher wind speeds and more frequent cut-out events in colder months, the most frequent and severe price spikes are experienced during the summer when electricity demand is the highest throughout the year. The summer price spikes are not due to excessive wind speeds; on the contrary, they are caused by sudden losses of wind power due to very low wind speeds as well as sudden drops in wind speeds.

Overall, we find that sudden losses of wind power due to extremely high wind speeds may not pose a major vulnerability to the ISO-NE bulk electricity grid. These validate the previously stated benefits of wind power during winter storms and could allow system planners to de-prioritize the possible threat of very high wind speeds during cold snaps. Nevertheless, enhanced reserve requirements, quick ramp capabilities (including from energy storage), and demand response practices should be adopted in order to increase the system's reliability to power loss related to both very high and very low wind speeds. The results from this study should prove valuable to stakeholders of electricity grids including ISO-NE, as well as researchers who focus on the risks of integrating variable renewable energy to the power grid under multivariate uncertainties and growing stresses, especially those related to extreme weather events related to

climate change. The is growing societal concern and scientific interest in the impacts of extreme weather events, which are becoming more frequent and severe with climate change, on bulk electricity grids. Much more future research is needed to better understand these vulnerabilities and identify mitigation strategies that complement the grid's dual objective of rapid decarbonization.

REFERENCES

Archer, C. L., Simão, H. P., Kempton, W., Powell, W. B., & Dvorak, M. J. (2017). The challenge of integrating offshore wind power in the U.S. electric grid. Part I: Wind forecast error. *Renewable Energy*, *103*, 346–360. https://doi.org/10.1016/j.renene.2016.11.047

Barthelmie, R. J., & Pryor, S. C. (2014). Potential contribution of wind energy to climate change mitigation. *Nature Climate Change*, *4*(8), 684–688. https://doi.org/10.1038/nclimate2269

Bessa, R., Moreira, C., Silva, B., & Matos, M. (2014). Handling renewable energy variability and uncertainty in power systems operation. *Wiley Interdisciplinary Reviews: Energy and Environment*, *3*(2), 156–178. https://doi.org/10.1002/wene.76

Bureau of Ocean Energy Management. (2018). *Vineyard Wind Offshore Wind Energy Project Draft Environmental Impact Statement*. https://www.boem.gov/sites/default/files/renewable-energy-program/State-Activities/MA/Vineyard-Wind/Vineyard_Wind_Draft_EIS.pdf

Cai, X., Qin, Z., & Hou, Y. (2018). Improving wind power utilisation under stormy weather condition by risk-limiting unit commitment. *IET Renewable Power Generation*, *12*(15), 1778–1785. https://doi.org/10.1049/iet-rpg.2018.5447

Chowdhury, A. F. M. K., Kern, J., Dang, T. D., & Galelli, S. (2020). PowNet: A Network-Constrained Unit Commitment/Economic Dispatch Model for Large-Scale Power Systems Analysis. *Journal of Open Research Software*, *8*. https://doi.org/10.5334/jors.302

Conejo, A. J., & Baringo, L. (2018). *Power System Operations*. Springer International Publishing. https://doi.org/10.1007/978-3-319-69407-8

EIA. (2018). *Household winter heating in the Northeast*. https://www.eia.gov/special/heatingfuels/images/WHF_longformat_01302018.pdf

EIA. (2019). *Table 7.1. Receipts, Average Cost, and Quality of Fossil Fuels for the Electric Power Industry, 2009 through 2019*. https://www.eia.gov/electricity/annual/html/epa_07_01.html

EIA. (2020a). *Units for comparing energy*. https://www.eia.gov/energyexplained/units-and-calculators/

EIA. (2020b). *Wind explained*. https://www.eia.gov/energyexplained/wind/electricity-generation-from-wind.php

EIA. (2021a). *Form EIA-923 detailed data with previous form data (EIA-906/920)*. https://www.eia.gov/electricity/data/eia923/

EIA. (2021b). *New York Harbor No. 2 Heating Oil Spot Price FOB*. https://www.eia.gov/dnav/pet/hist/eer_epd2f_pf4_y35ny_dpgD.htm

EIA. (2021c). *Weekly Heating Oil and Propane Prices (October - March)*. https://www.eia.gov/dnav/pet/pet_pri_wfr_a_EPD2F_PWR_dpgal_w.htm

EIA. (2021d). *Wholesale Electricity and Natural Gas Market Data*. https://www.eia.gov/electricity/wholesale/#history

EPA. (2020). *Emissions & Generation Resource Integrated Database (eGRID)*. https://www.epa.gov/egrid

Gualtieri, G., & Secci, S. (2011). Comparing methods to calculate atmospheric stability-dependent wind speed profiles: A case study on coastal location. *Renewable Energy*, *36*(8), 2189–2204. https://doi.org/10.1016/j.renene.2011.01.023

Gualtieri, G., & Secci, S. (2012). Methods to extrapolate wind resource to the turbine hub height based on power law: A 1-h wind speed vs. Weibull distribution extrapolation comparison. *Renewable Energy*, *43*, 183–200. https://doi.org/10.1016/j.renene.2011.12.022

Herman, J. D., Ph, D., Asce, A. M., Zeff, H. B., Ph, D., Lamontagne, J. R., Ph, D., Reed, P. M., Ph, D., Asce, A. M., Characklis, G. W., Ph, D., & Asce, M. (2016). *Synthetic Drought Scenario Generation to Support Bottom-Up Water Supply Vulnerability Assessments*. *142*(11), 1–13. https://doi.org/10.1061/(ASCE)WR.1943-5452.0000701.

ISO New England. (2018). *High-Level Assessment of Potential Impacts of Offshore Wind Additions to the New England Power System During the 2017-2018 Cold Spell*. https://www.iso-ne.com/static-assets/documents/2018/12/2018_iso-ne_offshore_wind_assessment_mass_cec_production_estimates_12_17_2018_public.pdf

ISO New England. (2020a). *Resource Mix*. https://www.iso-ne.com/about/key-stats/resource-mix/

ISO New England. (2020b). *Ties to Neighboring Grids*. https://www.iso-ne.com/about/key-stats/maps-and-diagrams

ISO New England. (2021a). *Daily Generation by Fuel Type*. https://www.iso-ne.com/isoexpress/web/reports/operations/-/tree/daily-gen-fuel-type

ISO New England. (2021b). *Energy, Load, and Demand Reports*. https://www.iso-ne.com/isoexpress/web/reports/load-and-demand/-/tree/zone-info

ISO New England. (2021c). *External Interface Metered Data*. https://www.iso-ne.com/isoexpress/web/reports/grid/-/tree/external-interface-metered-data

ISO Newswire. (2018). *Winter 2017/2018 recap: Historic cold snap reinforces findings in Operational Fuel-Security Analysis*. http://isonewswire.com/updates/2018/4/25/winter-20172018-recap-historic-cold-snap-reinforces-findings.html

Lall, U., & Sharma, A. (1996). A nearest neighbor bootstrap for resampling hydrologictime series. *Water Resources Research*, *32*(3), 679–693. https://doi.org/10.1029/95WR02966

Lin, J., Sun, Y., Cheng, L., & Gao, W. (2012). Assessment of the power reduction of wind farms under extreme wind condition by a high resolution simulation model. *Applied Energy*, *96*, 21–32. https://doi.org/10.1016/j.apenergy.2011.10.028

Lin, X., Wang, Z., Ding, S., Zhang, Z., & Li, Z. (2019). A power output and mechanical model of a wind turbine and its control strategy under severe wind conditions. *Journal of Renewable and Sustainable Energy*, *11*(4), 043303. https://doi.org/10.1063/1.5088666

Masters, G. M. (2013). *Renewable and efficient electric power systems* (2. edition). John Wiley & Sons.

MHI Vestas Offshore Wind. (2017). *The world's most powerful available wind turbine gets major power boost*. https://mhivestasoffshore.com/worlds-most-powerful-available-wind-turbine-gets-major-power-boost/

Muzhikyan, A., Muhanji, S. O., Moynihan, G. D., Thompson, D. J., Berzolla, Z. M., & Farid, A. M. (2019). The 2017 ISO New England System Operational Analysis and Renewable Energy Integration Study (SOARES). *Energy Reports*, *5*, 747–792. https://doi.org/10.1016/j.egyr.2019.06.005

NASEM. (2021). *Accelerating Decarbonization of the U.S. Energy System*. National Academies Press. https://doi.org/10.17226/25932

National Weather Service. (2021). *What Are Heating and Cooling Degree Days*. https://www.weather.gov/key/climate_heat_cool

NOAA. (2021). *Local Climatological Data (LCD)*. https://www.ncdc.noaa.gov/cdo-web/datatools/lcd

Ren, G., Wan, J., Liu, J., Yu, D., & Söder, L. (2018). Analysis of wind power intermittency based on historical wind power data. *Energy*, *150*, 482–492.

https://doi.org/10.1016/j.energy.2018.02.142

Sahin, A. D., & Sen, Z. (2001). First-order Markov chain approach to wind speed modelling. *Journal of Wind Engineering and Industrial Aerodynamics*, *89*(3–4), 263–269. https://doi.org/10.1016/S0167-6105(00)00081-7

Solaun, K., & Cerdá, E. (2019). Climate change impacts on renewable energy generation. A review of quantitative projections. *Renewable and Sustainable Energy Reviews*, *116*, 109415. https://doi.org/10.1016/j.rser.2019.109415

Speake, A., Donohoo-Vallett, P., Wilson, E., Chen, E., & Christensen, C. (2020). Residential Natural Gas Demand Response Potential during Extreme Cold Events in Electricity-Gas Coupled Energy Systems. *Energies*, *13*(19), 5192. https://doi.org/10.3390/en13195192

Su, C., Hu, W., Chen, Z., & Hu, Y. (2013). Mitigation of power system oscillation caused by wind power fluctuation. *IET Renewable Power Generation*, *7*(6), 639–651. https://doi.org/10.1049/iet-rpg.2012.0253

The Wind Power. (2021). *V164/9500*. https://www.thewindpower.net/turbine_en_1476_mhi-vestas-offshore_v164-9500.php

Turconi, R., O'Dwyer, C., Flynn, D., & Astrup, T. (2014). Emissions from cycling of thermal power plants in electricity systems with high penetration of wind power: Life cycle assessment for Ireland. *Applied Energy*, *131*, 1–8. https://doi.org/10.1016/j.apenergy.2014.06.006

Wang, J., Qin, S., Jin, S., & Wu, J. (2015). Estimation methods review and analysis of offshore extreme wind speeds and wind energy resources. *Renewable and Sustainable Energy Reviews*, *42*, 26–42. https://doi.org/10.1016/j.rser.2014.09.042

World Meteorological Organization. (2008). *Guide to Meteorological Instruments and Methods*

of Observation. https://www.weather.gov/media/epz/mesonet/CWOP-WMO8.pdf

Zhang, D., Xu, Z., Li, C., Yang, R., Shahidehpour, M., Wu, Q., & Yan, M. (2019). Economic and sustainability promises of wind energy considering the impacts of climate change and vulnerabilities to extreme conditions. *Electricity Journal*, *32*(6), 7–12. https://doi.org/10.1016/j.tej.2019.05.013

APPENDICES

APPENDIX A. Completing Missing Hourly Wind Speed Data at Project Site

In order to fill the missing hourly wind speed data at Vineyard Wind site, every day with a complete, 24-hour record was selected. For these days, the ratio of hourly wind speeds to maximum hourly wind speed was found, creating a 24-hour daily profile of values between 0 and 1. We then examined the entire daily wind speed record, performing a different operation on each day, depending on the number of missing hours. If the specific day contains 1-11 hours of missing data, missing hourly values are linearly interpolated. On the other hand, if the specific day contains 12-24 hours of missing data, a 24-hour profile is randomly sampled from a different day within the same month. The selected profile is multiplied by the daily max wind speed for the current day.

APPENDIX B. Downscaling Synthetic Daily to Hourly Wind Speeds at Vineyard Wind Site

Hourly wind speed values for the extended 1949-2016 dataset are calculated as follows. First, using the observed hourly Vineyard Wind data for 2016-2018, we determine hourly wind fraction profiles for each day, found by dividing every hourly wind speed on a specific day by the sum of every hourly wind speed on that day. For the extended 1949-2016 data set, daily wind speeds are compared alongside the 2016-2018 observed record and the closest match is determined in terms of absolute difference. For the selected day, total wind speed is found by multiplying daily wind speed by 24 hours. Then, the hourly profile for the identified day is used to determine hourly values for the day in the extended dataset. Again, observed values for 2016-2018 are added to the end and this gives us hourly wind speeds at the Vineyard Wind site over the period 1949-2018 at every hub height.

APPENDIX C. Modeling electricity demand

There are eight load zones in the ISO-NE market: Maine (ME), Vermont (VT), New Hampshire (NH), Western/Central Massachusetts (WCMA), Northeast Massachusetts (NEMA), Southeast Massachusetts (SEMA), Rhode Island (RI) and Connecticut (CT). To simulate demand in each zone and the overall system, hourly real-time loads for these zones are gathered between 2011-2018 from ISO Express (ISO New England, 2021b), and daily peak demand values are extracted over this time period.

In general, electricity demand has a non-linear relationship with air temperatures. Both very low and very high temperatures increase demand, while mild temperatures decrease it (see Figure 4a). Wind speeds also have a somewhat complex relationship with electricity demand; on low temperature days, high wind speeds tend to increase demand, while high wind speeds on hot days tend to decrease it. In order to account for these non-linear relationships, daily records of temperature and wind speeds at each of seven weather stations are split based on heating degree days (HDD) and cooling degree days (CDD). Degree days are calculated by looking at the absolute value difference between average daily temperature and 65 °F. It is assumed that given the ambient temperature is 65 °F, no heating or cooling is needed (National Weather Service, 2021). The impact of wind speeds in HDDs or CDDs is estimated by using the below approach:

$$WHDD_d = \begin{cases} 0, & if\ HDD = 0 \\ WS_d, & if\ HDD > 0 \end{cases} \quad \text{(S1)}$$

$$WCDD_d = \begin{cases} 0, & if\ CDD = 0 \\ WS_d, & if\ CDD > 0 \end{cases} \quad \text{(S2)}$$

Where,

$WHDD_d$ = wind speed (given heating demands) on day d (m/s)

$WCDD_d$ = wind speed (given cooling demands) on day d (m/s)

WS_d = average wind speed on day d (m/s)

Temperature data is disintegrated into 5 degrees Fahrenheit portions between 80 °F and 10 °F to represent them as linear models. Records of degree days, associated wind speeds for all meteorological stations, and day of week (workday or weekend) are used as independent variables in multivariate regressions of daily peak electricity demand for each of the eight ISO-NE zones. The multivariate regressions are trained on historical weather and daily peak electricity demand data over the period 2011-2018. This approach is able to produce estimates of daily peak electricity demand (Figure 4b). Moreover, logical bounds are used to prevent the model from overestimating or underestimating by using historical daily peak electricity demand data. Residuals are simulated by using a VAR model and added to estimated values to have a complete dataset of daily peak electricity demand estimates between 1949 and 2018.

After simulating daily peak electricity demand for each zone, hourly electricity demand is determined by multiplying peak demands with 24-hour load profiles for each zone and each calendar day. These profiles, which are calculated using historical data, represent the typical fraction of daily peak demand experienced in each hour.

APPENDIX D. Modeling Interchange Flows with Adjacent Systems

There are six main interchange lines between the ISO-NE market and the external systems. Those are connected to New York (ROSETON, SHOREHAM, and NORTHPORT), Hydro Québec (HQ_P1_P2 and HQHIGATE), and New Brunswick (SALBRYNB). Daily net interchange data for those six lines are gathered between 2012-2018 from ISO Express (ISO New England, 2021c).

Since daily interchange is somewhat affected by electricity demand, an approach similar to electricity demand modeling is adopted. Wind speed and temperature data from seven weather stations are split into HDDs and CDDs and the impact of wind speeds in HDDs or CDDs is estimated by using the same approach (see S1 and S2). Net interchange values are separated with respect to months and represented as linear models.

Records of degree days, associated wind speeds for all meteorological stations, and day of week (workday or weekend) are used as independent variables in multivariate regressions of daily net interchange for each of the six interchange lines. The multivariate regressions are trained on historical weather and daily net interchange data over the period 2012-2018. This approach is able to produce estimates of daily net interchange (Figure 4c). Moreover, logical bounds are used to prevent the model from overestimating or underestimating by using historical daily net interchange data. Residuals are simulated by using VAR model and added to estimated values to have a complete dataset of daily net interchange estimates between 1949 and 2018.

APPENDIX E. UC/ED Model Inputs and Their Usage

In this section, UC/ED model inputs and their place in the model's working mechanism are explained in detail. Model inputs consist of generator information, hourly demand, daily dispatchable imports, hourly exports, hourly solar, hourly onshore wind, hourly offshore wind, daily dispatchable hydropower, interchange line limits (both within internal nodes and external systems), and fuel prices.

E.1. Generator Information

All generators operating in the ISO-NE market in 2018 and their related information are gathered from Emissions & Generation Resource Integrated Database (eGRID) (EPA, 2020). From the dataset, dispatchable generators are divided into coal, natural gas, oil, imports, and hydropower. By using the information from eGRID and the industry standards, the model is fed with generator names, types, zones, net capacities in MW, heat rates in MMBtu/MWh, minimum capacities in MW, ramping capacities in MW, minimum up and down times in hours, no load costs in USD, variable operation and maintenance costs in USD/MWh, and startup costs in USD. Furthermore, to every load zone, one slack generator, an unreasonably expensive unit that would only be used as a last resort, is added to prevent blackout scenarios that could impede model runs.

On the other hand, nuclear, municipal solid waste, landfill gas, and wood waste plants are regarded differently. Average electricity generation in 2018 from those plants is fed to the model as a zonal must-run time series. To prevent the model from overproducing electricity, a minor price in USD/MWh is set for the must-run generation.

Moreover, the reserve requirement of the system is assumed to 4% of the hourly total demand and the model schedules non-spinning reserves from thermal generators for this purpose.

E.2. Imports and Exports

From the daily net interchange estimates between 1949 and 2018, net import days and net export days are separated as follows (Positive net interchange values represent net import days, and negative net interchange values represent net export days):

$$Imports_{i,j} = \begin{cases} 0, & Path_{i,j} < 0 \\ Path_{i,j}, & otherwise \end{cases} \quad \text{(S3)}$$

$$Exports_{i,j} = \begin{cases} 0, & Path_{i,j} > 0 \\ Path_{i,j}, & otherwise \end{cases} \quad \text{(S4)}$$

Where,

$Imports_{i,j}$ = imports on path i on day j (MWh)

$Path_{i,j}$ = power flows on path i on day j (MWh)

$Exports_{i,j}$ = exports on path i on day j (MWh)

By utilizing this approach, daily total import time-series are created. Daily total import availability is distributed to the zones by using the interchange line details (ISO New England, 2020b). The model dispatches available daily imports optimally by using a UC/ED approach.

For the exports, daily and hourly net interchange data between 2008-2018 are gathered from ISO Express (ISO New England, 2021c). Net import/export days and hours are distinguished with the same method (see S3 and S4). Net export hours are divided by the total exports on that day in order to create an hourly export profile for each interchange line. By taking the average of those hourly profiles in different years, a 365-day hourly export profile is generated. Missing days are filled by copying the nearest day's hourly profile. These profiles are multiplied by the net daily export values to come up with a 69 years time-series of hourly exports. Hourly exports are

distributed to the zones by using the interchange line details (ISO New England, 2020b) as well as interchange line limits.

It is assumed that imports cost per MWh is the same as the cheapest thermal generator's generation cost. Therefore, a cost of 4.3 USD/MWh is used in the UC/ED process for the imports. This assumption is utilized to preclude the model from over generating electricity as well as to make sure that extent of import usage in the system is as similar as possible to the ISO-NE market.

E.3. Solar and Wind Power

Solar and onshore wind generation data for the ISO-NE market in 2018 is collected from ISO Express (ISO New England, 2021a) and used for every simulation year. Since the data consist of total generation in the system, available generation is distributed among eight zones with respect to solar and onshore wind capacity ratios of those zones. Capacity ratios are found by taking the ratio of individual zone's solar and offshore wind capacity and total solar and offshore wind capacity of the ISO-NE market. The capacity information is gathered from 2018 eGRID dataset. The model dispatches or curtails available solar and offshore wind power optimally by considering numerous system conditions.

Offshore wind power is simulated for 69 years as discussed before and a time series of available offshore wind power for different hub heights are fed to the model. All offshore wind power is connected to SEMA because Vineyard Wind is going to be interconnected to Barnstable Switching Station in SEMA zone (Bureau of Ocean Energy Management, 2018). The model dispatches or curtails available offshore wind power optimally by considering numerous system conditions.

E.4. Hydropower

Monthly hydropower generation data between 2011 and 2018 is collected from U.S. Energy Information Administration (EIA, 2021a). Hydropower generators in this data are matched with 2018 eGRID dataset and net monthly generation from those generators are accumulated into eight zones. By taking the average of zonal hydropower generation in different years, a 12-month available hydropower time series is generated. Monthly hydropower is divided equally into days. Consequently, a 365-day available hydropower time series is created for each zone and used for every simulation year.

By using the capacities in 2018 eGRID dataset, zonal hydropower generators are produced and added to the generators file. The model uses these generators and daily available hydropower time series to dispatch hydropower optimally.

E.5. Fossil Fuel Prices

Average daily natural gas prices at Algonquin Citygates between 2015 and 2017 are assembled from EIA Wholesale Electricity and Natural Gas Market Data (EIA, 2021d). Few missing daily data is filled with linear interpolation. By taking the average of daily natural gas prices in different years, a 365-day natural gas price time series is generated and used for every simulation year. This approach is used in order to capture and use the natural gas price trend in New England (high prices in winter, low prices in summer) in the model.

For the oil prices, a linear regression model is developed between New York Harbor heating oil prices and wholesale heating oil prices in the New England states. Daily New York Harbor No. 2 heating oil spot prices and weekly heating oil prices in the six states of the ISO-NE market between 2015 and 2018 are accumulated from EIA Petroleum & Other Liquids data (EIA,

2021b, 2021c). Few missing daily data is completed with linear interpolation. Moreover, New York Harbor prices are filtered with respect to dates included in weekly heating oil prices, and a linear regression model is used between these two to come up with daily heating oil prices in the eight zones between 2015-2018 (with an R^2 of 0.94). Oil prices in SEMA, WCMA, and NEMA are considered the same as the price in Massachusetts. Since 1 gallon of heating oil contains 138,500 Btu energy (EIA, 2020a), the fuel price for oil generators (in USD/MMBtu) is computed by dividing gallon prices by 0.1385. By taking the average of daily oil prices in different years, a 365-day oil price time series is generated and used for every simulation year.

Coal price is assumed to be static and taken as 2.2 USD/MMBtu. This is the average coal price in the U.S. between 2009-2018 (EIA, 2019).

E.6. Formulation of UC/ED Model

In this study, New England electricity market operations are analyzed by using the Unit Commitment/Economic Dispatch (UC/ED) modeling approach in terms of reliability under extreme weather events and offshore wind integration. In Unit Commitment (UC), power plants' commitment is decided by taking electricity demand and security constraints into account. On the other hand, in Economic Dispatch (ED), power output from all online power plants is determined while trying to minimize system costs and meet constraints about transmission and other technical aspects (Conejo & Baringo, 2018). To put it simply, UC decides which power plants to start operating and which power plants to stop operating in a specified timeframe whereas ED determines the electricity to be generated by each power plant in the grid (Chowdhury et al., 2020). Our UC/ED model of ISO-NE system utilizes mixed-integer linear programming and simulates the system operations in an iterative manner.

E.6.1. Decision Variables

The UC/ED model contains both binary and continuous decision variables, which are electricity generation amount from three heat rate segments of individual generators, "on/off" status of generators, amount of spinning and non-spinning reserves offered by each generator, renewable energy generation amount from solar, onshore and offshore wind, generation amount from must-run resources (nuclear, municipal solid waste, landfill gas plants, etc.) and power flow between eight load zones. Binary variables are employed to govern generator "on/off" status, and in turn controls the no load, and startup costs in the objective function. Continuous variables are utilized in order to decide electricity amount as well as reserves amount offered by each generator, which manages fuel and variable operation and maintenance (O&M) costs in the objective function. Other continuous variables govern electricity generation from renewable energy sources and must-run sources and electricity transfer between eight zones of the model topology.

E.6.2. Objective Function

The model's objective function tries to minimize the cost of meeting demand for electricity and operating reserves in the ISO-NE market for every hour along the operating horizon:

$$Objective\ Function = \sum_{t=1}^{T} \sum_{j}^{J} \sum_{z}^{Z} (Fuel\ Costs_{t,j,z} + Variable\ O\&M\ Costs_{t,j,z} + No\ Load\ Costs_{t,j,z} + Start\ Costs_{t,j,z}) + \sum_{t=1}^{T} \sum_{s}^{S} \sum_{k}^{K} Power\ Flow\ Costs_{t,s,k} \quad \text{(S5)}$$

Where,

t ∈ operating horizon $\{1 \dots T\}$

z ∈ set Z of zones $\{CT, ME, NEMA, NH, RI, SEMA, VT, WCMA\}$

j ∈ set J of generators $\{coal1, coal2, gas1, gas2, oil1, oil2 \ldots J\}$

s ∈ set S of zones $\{CT, ME, NEMA, NH, RI, SEMA, VT, WCMA\}$

k ∈ set K of zones $\{CT, ME, NEMA, NH, RI, SEMA, VT, WCMA\}$

Individual elements of the objective function are itemized below:

$$Fuel\ Costs_{t,j,z} = FP \times (P1_{j,z,t} \times S1_{j,z} + P2_{j,z,t} \times S2_{j,z} + P3_{j,z,t} \times S3_{j,z}) \quad \text{(S6)}$$

$$Variable\ O\&M\ Costs_{t,j,z} = (P1_{j,z,t} + P2_{j,z,t} + P3_{j,z,t}) \times VC_{j,z} \quad \text{(S7)}$$

$$No\ Load\ Costs_{t,j,z} = ON_{j,z,t} \times NL_{j,z} \quad \text{(S8)}$$

$$Start\ Costs_{t,j,z} = SWITCH_{j,z,t} \times SC_{j,z} \quad \text{(S9)}$$

$$Power\ Flow\ Costs_{t,s,k} = FLOW_{s,k,t} \times Hurdle_{s,k} \quad \text{(S10)}$$

Where,

$P1_{j,z,t}$ = power produced in 1st heat rate segment of generator j in zone z in hour t (MWh)

$P2_{j,z,t}$ = power produced in 2nd heat rate segment of generator j in zone z in hour t (MWh)

$P3_{j,z,t}$ = power produced in 3rd heat rate segment of generator j in zone z in hour t (MWh)

$ON_{j,z,t}$ = binary; 1 if generator j in zone z is on in hour t; 0 otherwise

$SWITCH_{j,z,t}$ = binary; 1 if generator j in zone z starts in hour t; 0 otherwise

$FLOW_{s,k,t}$ = power flow from zone s to zone k in hour t (MWh)

FP = fuel price (USD/MMBtu)

$S1_{j,z}$ = marginal heat rate for 1st capacity segment of generator j in zone z (MMBtu/MWh)

$S2_{j,z}$ = marginal heat rate for 2nd capacity segment of generator j in zone z (MMBtu/MWh)

$S3_{j,z}$ = marginal heat rate for 3rd capacity segment of generator j in zone z (MMBtu/MWh)

$VC_{j,z}$ = variable O&M cost for generator j in zone z (USD/MWh)

$NL_{j,z}$ = no load cost for generator j in zone z (USD)

$SC_{j,z}$ = startup cost of generator j in zone z (USD)

$Hurdle_{s,k}$ = hurdle rate on power flows from zone s to zone k (USD/MWh)

E.6.3. Constraints

The objective function is bounded by various constraints on each generator and in addition to constraints on power balance and power flow between load zones. For instance, there is a zero-sum constraint to make sure that the summation of power produced, and reserves do not exceed the maximum capacity for each generator. Moreover, there is a constraint that limits the hourly power generation fluctuations with predetermined ramp rates. Another constraint is set to make sure that generators abide by predetermined minimum up (online) and down (offline) hours. On the larger side, there are constraints ensuring at least 25% of the electricity demand is supplied by generators within that zone, and constraints restricting the power flow to individual line limits between each zone. Lastly, an energy balance constraint is utilized to ensure that sum of power generated within a zone and imports to that zone are equal to the sum of the demand of that zone and exports from that zone. Energy balance constraint is detailed below:

$$\sum_z^Z(\sum_{j=1}^J(P1_{j,z,t} + P2_{j,z,t} + P3_{j,z,t}) + Imports_{z,t} + \sum_{s=1}^S FLOW_{s,z,t}) =$$

$$\sum_z^Z(Demand_{z,t} + Exports_{z,t} + \sum_{k=1}^K FLOW_{z,k,t}) \quad \text{(S11)}$$

Where,

$Imports_{z,t}$ = imports into zone z from outside the eight load zones in hour t (MW)

$Demand_{z,t}$ = electricity demand in zone z in hour t (MW)

$Exports_{z,t}$ = exports from zone z to outside the eight load zones in hour t (MW)

$FLOW_{s,z,t}$ = power flow from zone s to zone z in hour t (MW)

$FLOW_{z,k,t}$ = power flow from zone z to zone k in hour t (MW)

APPENDIX F. Validation of the Model

The model is validated by using day-ahead locational marginal prices (DA-LMP) observed in the ISO-NE market between 2015 and 2017. DA-LMP data is collected from ISO Express (ISO New England, 2021b). For the validation, historical natural gas and oil prices are used rather than the 365-day fuel price time series. As the model generates DA-LMP data for eight load zones, an Elastic-Net linear regression model is developed to compute a time series that represents the overall DA-LMP at the ISO-NE system. The reasoning behind choosing the Elastic-Net model rather than an ordinary least squares model is to make sure that all regression coefficients are higher than zero to avoid negative prices as well as to represent every load zone in the overall price determination. This approach is able to accurately predict daily as well as hourly DA-LMP in the ISO-NE market (see Figure A1).

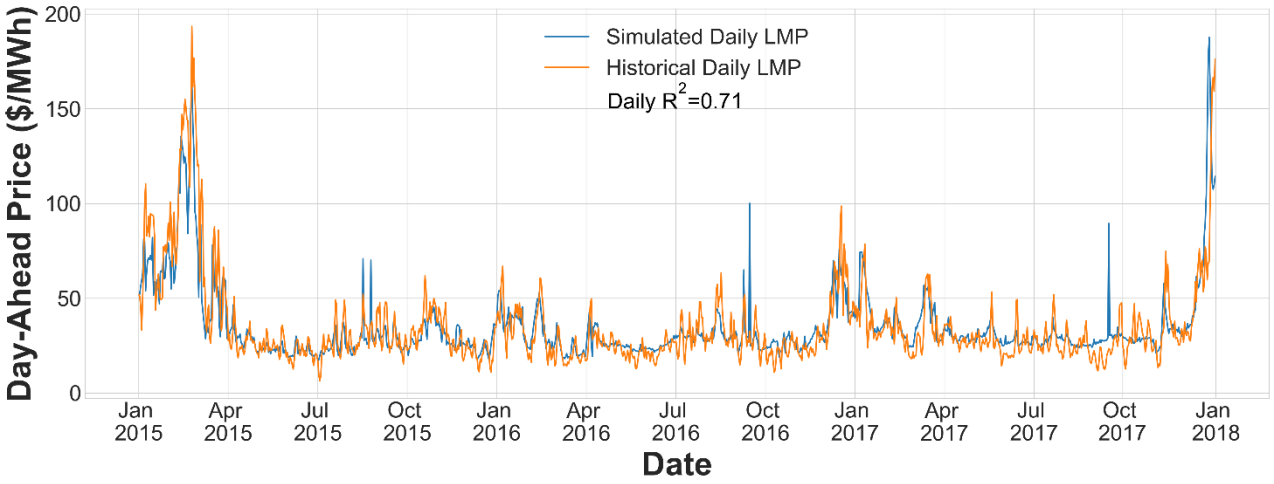

Figure A1: Comparison of historical and predicted daily day-ahead electricity price.

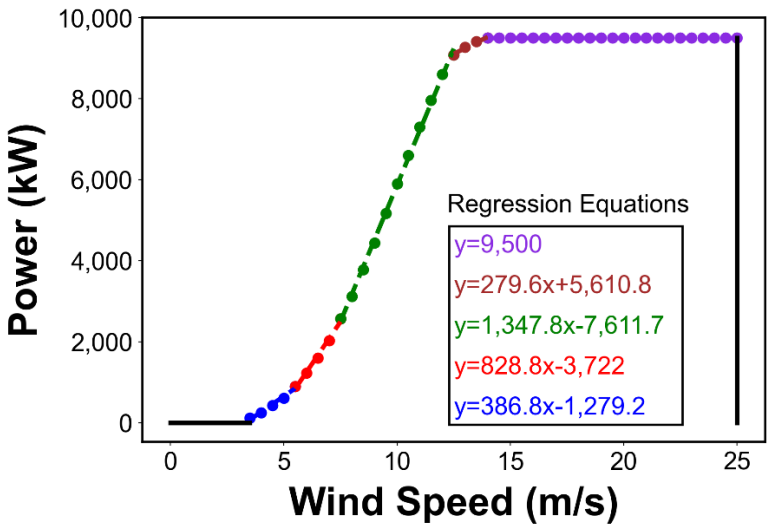

Figure A2: Five piecewise linear regression lines and related equations for MHI Vestas Offshore - V164.

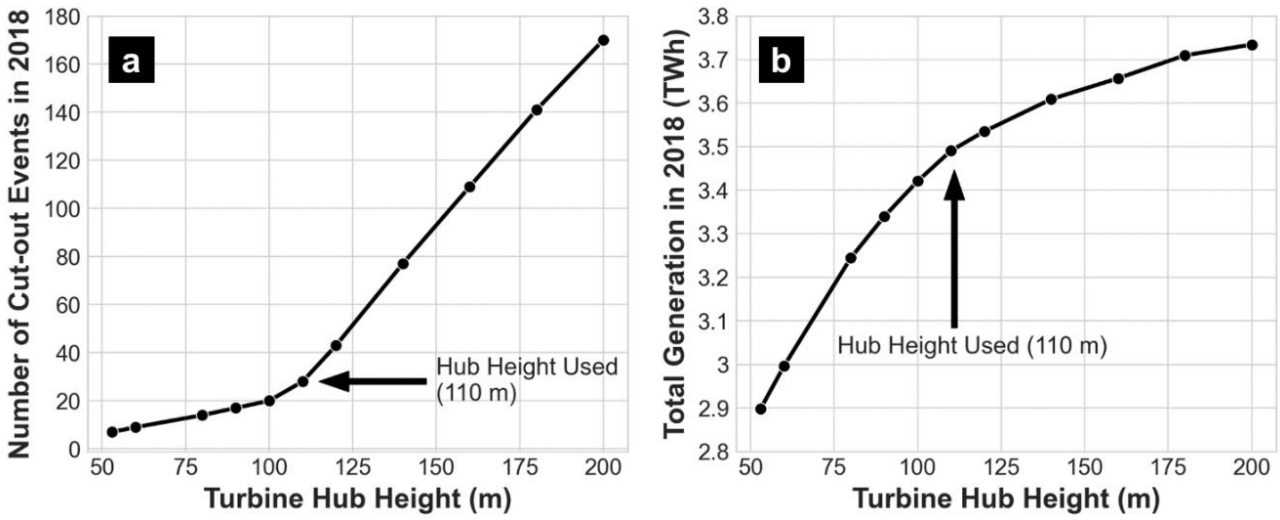

Figure A3: (a) Relationship between turbine hub height and frequency of cut-out events; (b) relationship between turbine hub height and annual electricity generation.

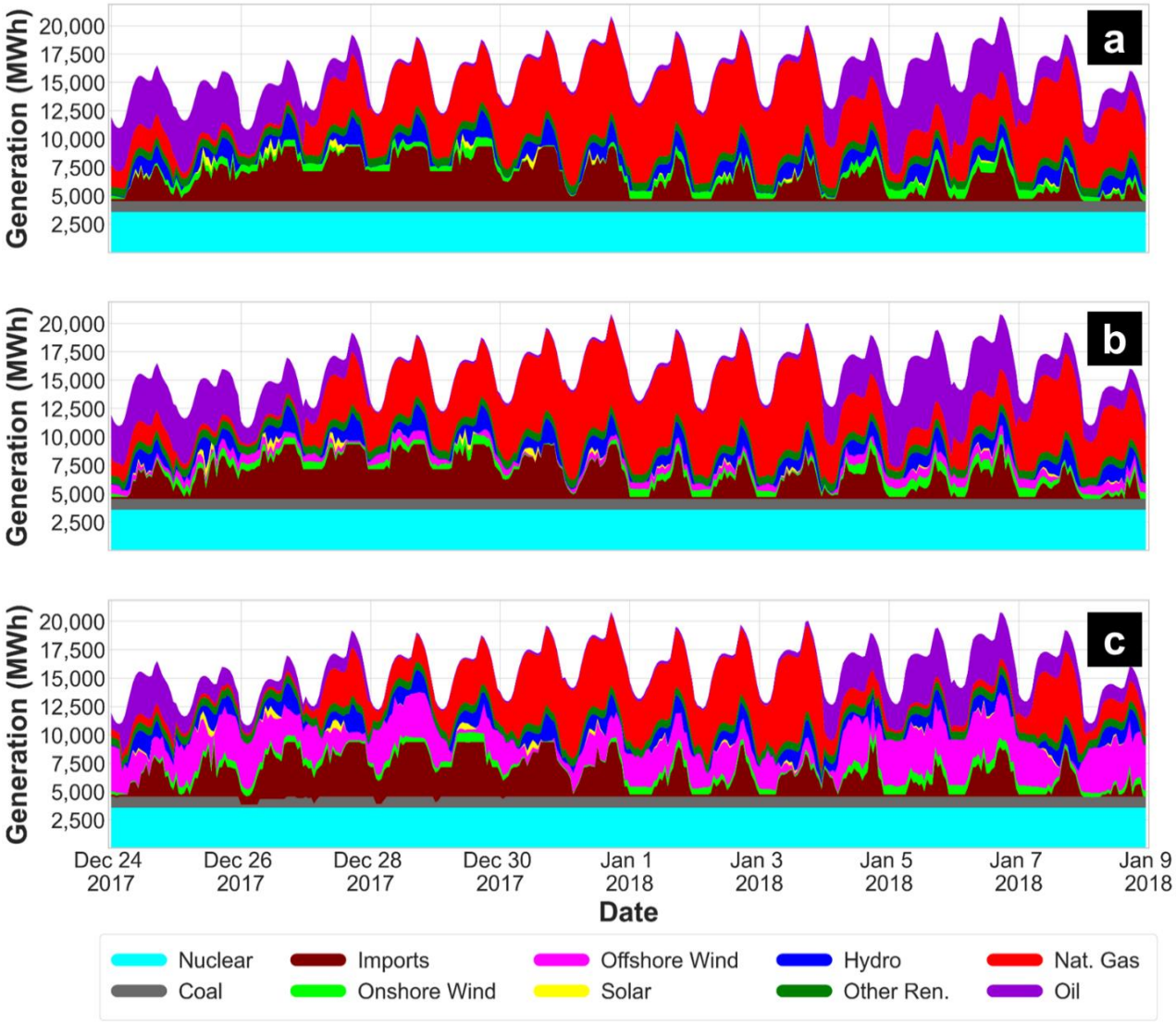

Figure A4: (a) Generation mix for 0 MW case during the cold snap; (b) generation mix for 800 MW case during the cold snap; (c) generation mix for 4,000 MW case during the cold snap.

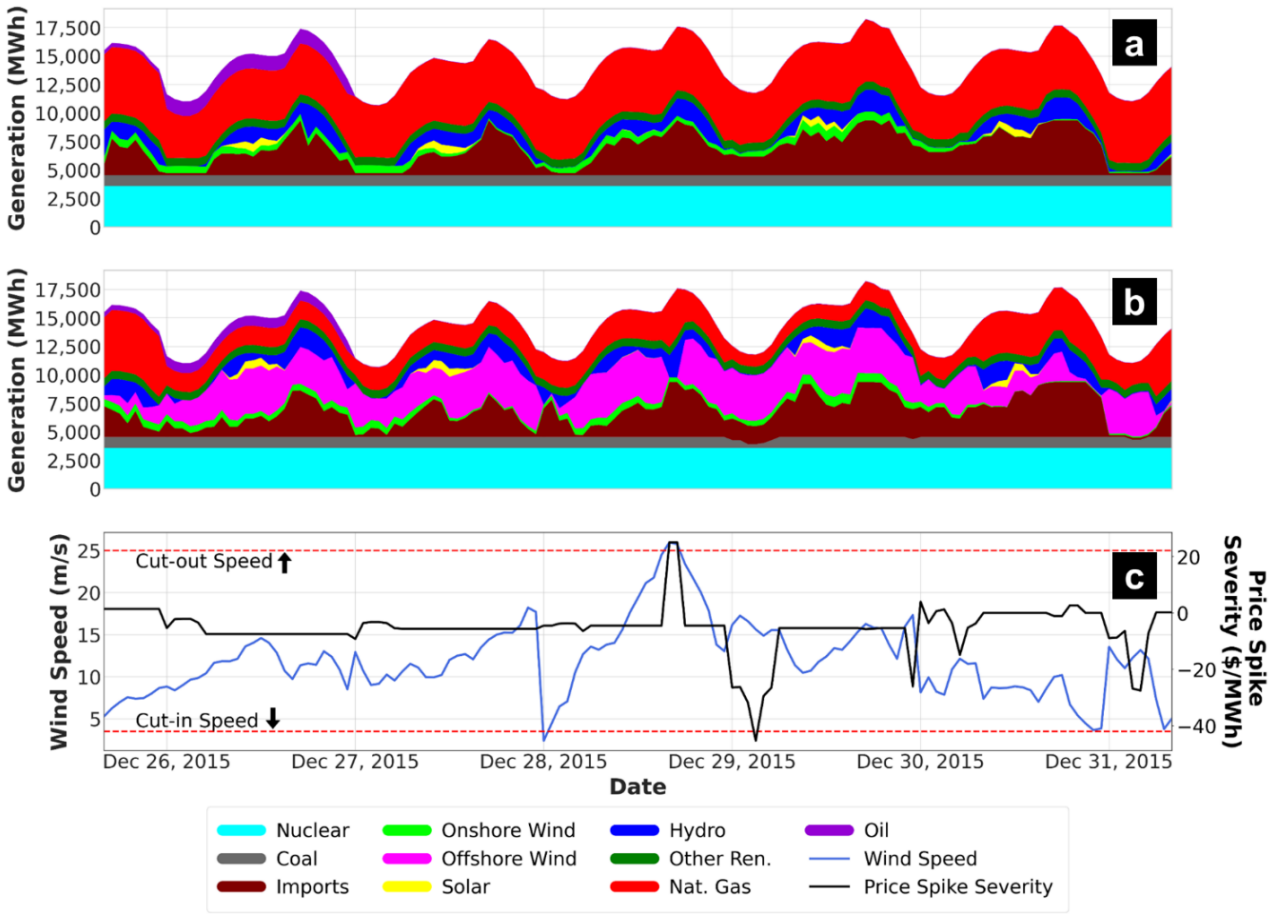

Figure A5: (a) Change in generation mix in 0 MW case in case of a cut-out event; (b) change in generation mix in 4,000 MW case in case of a cut-out event; (c) change in wind speed and price spike severity during a cut-out event. (Price spike severity is calculated by subtracting 0 MW case prices from 4,000 MW case prices.)

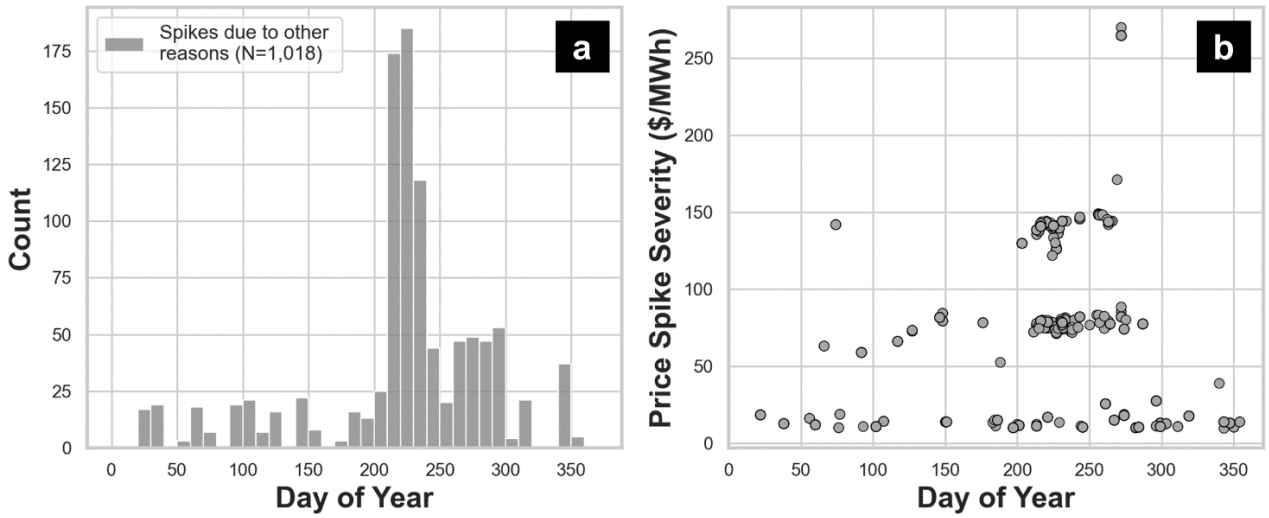

Figure A6: (a) Seasonality and reason for electricity price spikes in 800 MW case; (b) seasonality and magnitude of electricity price spikes in 800 MW case. Price spikes are calculated by subtracting prices under 0 MW from prices in other scenarios. Spikes are defined here as differences > $10/MWh. Gray designates spikes due to other reasons (low wind speeds), whereas red shows the spikes due to cut-out events.

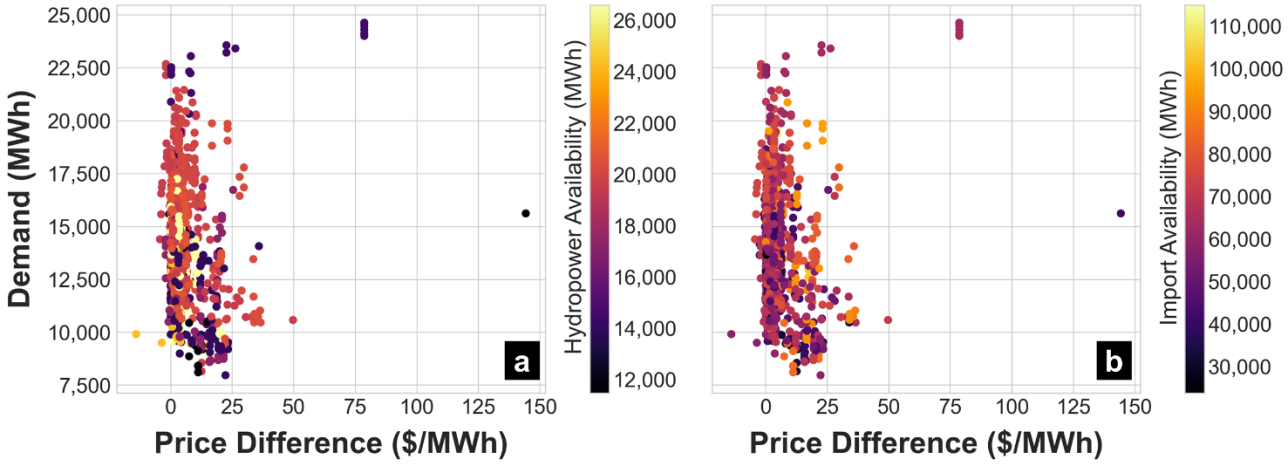

Figure A7: (a) Impact of demand and hydropower availability on the magnitude of price difference between 4,000 MW and 4,000 MW No Cut-out case during cut-out hours. (Price difference is calculated by subtracting 4,000 MW No Cut-out case prices from 4,000 MW case prices. Color designates the daily hydropower availability.); (b) impact of demand and import availability on the magnitude of price difference between 4,000 MW and 4,000 MW No Cut-out case during cut-out hours. (Price difference is calculated by subtracting 4,000 MW No Cut-out case prices from 4,000 MW case prices. Color designates the daily import availability.)

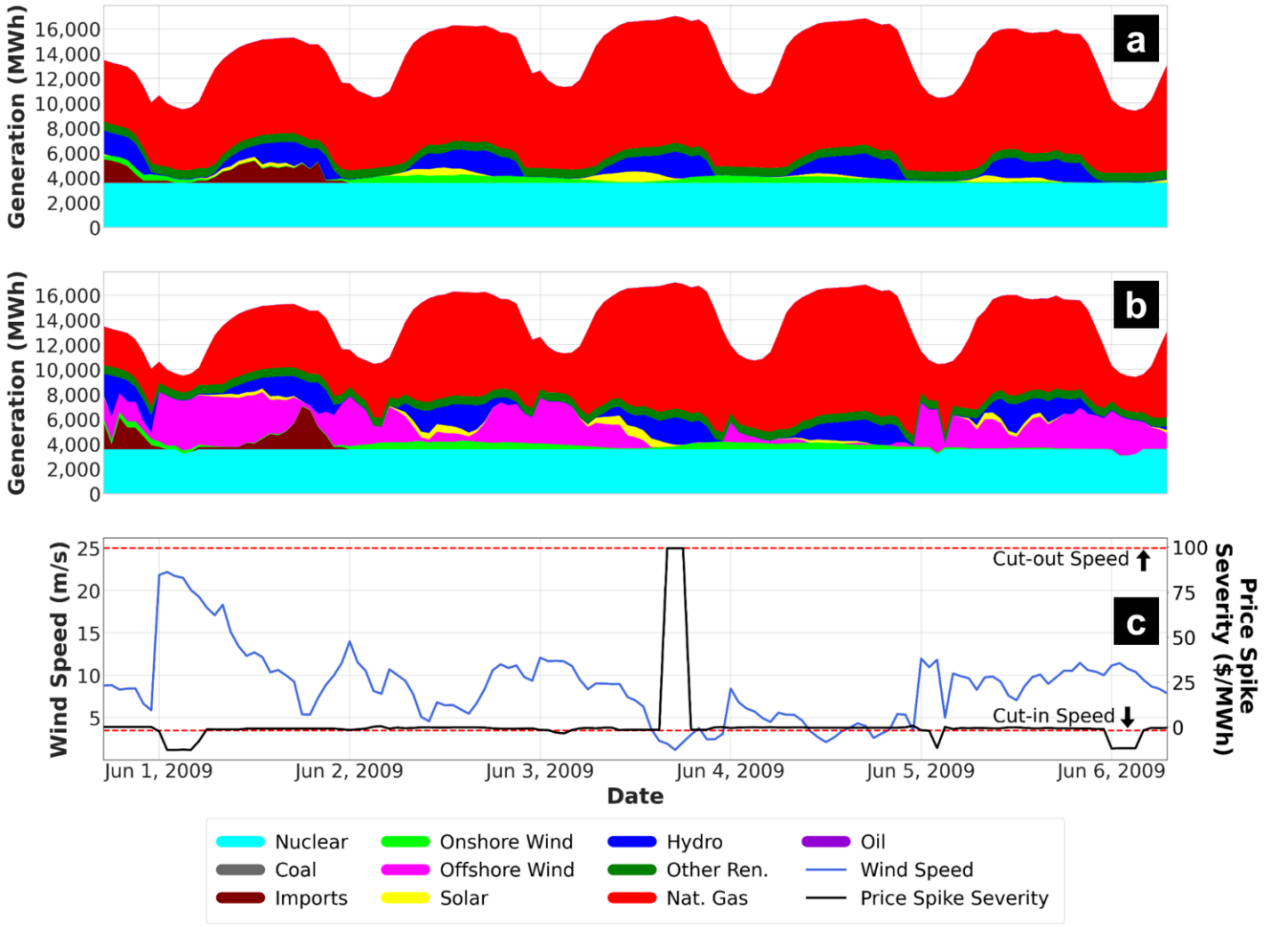

Figure A8: (a) Change in generation mix in 0 MW case during wind speeds lower than cut-in speed; (b) change in generation mix in 4,000 MW case during wind speeds lower than cut-in speed; (c) change in wind speed and price spike severity during wind speeds lower than cut-in speed. (Price spike severity is calculated by subtracting 0 MW case prices from 4,000 MW case prices.)

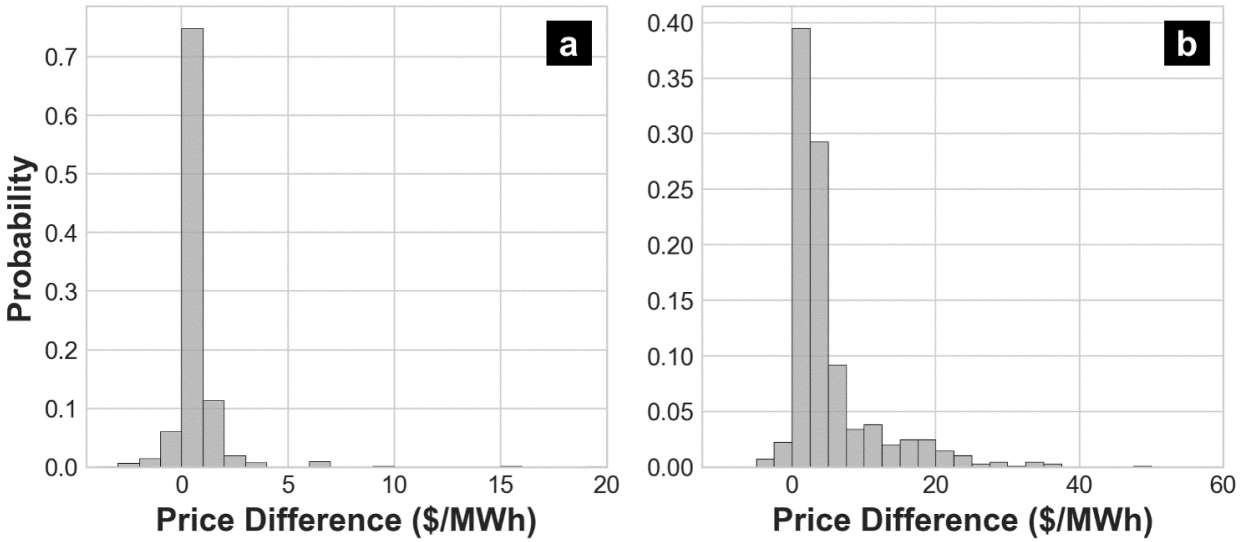

Figure A9: (a) Distribution of price differences between 800 MW and 800 MW No Cut-out cases during cut-out events. (Price difference is calculated by subtracting 800 MW No Cut-out case prices from 800 MW case prices); (b) distribution of price differences between 4,000 MW and 4,000 MW No Cut-out cases during cut-out events. (Price difference is calculated by subtracting 4,000 MW No Cut-out case prices from 4,000 MW case prices.)